ENGINEERING ARYLBORONATE – MODIFIED DEXTRAN POLYMERS FOR USE AS BIOCOMPATIBLE, BIODEGRADABLE MATERIALS IN MICROPARTICULATE IMMUNOTHERAPY

Amanda J. Manaster

A thesis presented to the faculty of Mount Holyoke College in partial fulfillment of the requirements for the degree of Bachelor of Arts with High Honors

Program in Biochemistry

South Hadley, Massachusetts

May 2019

This thesis was prepared
under the direction of Dr. Kyle Broaders
for eight credits

Acknowledgements

First, I'd like to thank my thesis advisor, Dr. Kyle Broaders for his invaluable support and guidance for the past two years. Thank you for creating a learning environment that inspires intellectual creativity and fuels productivity. Thank you for your patience throughout my entire journey in your lab and thank you for being willing to share your passion for organic chemistry and its promise in medicine with me.

Thank you to Emily Graham, my co-inaugural thesis student of the Broaders Lab. Experiencing this process with a comrade made a world of a difference and your self-motivation this past semester has been inspiring. Thank you Aiza Malik, you may not know it, but your advice and guidance at the very beginning of my time in the Broaders Lab has resonated with me since. Thank you, Annabelle Ooi, for laying the exploratory groundwork on this project several years ago and so graciously allowing me to join team Boron as you were transitioning into the next chapter of your life. Thank you, Sherry Yang, for your initial and continued work that has helped me expand my study to a more comprehensive survey on diol behavior. Thank you, Catherine Peabody, your bright energy in lab has kept me going this past few months. To the new Broaders Lab members, Maegan Windus, Abby Kaplan, Ariel Kimberly, and Tracy Zheng, thank you for tolerating my scatter-brained, mildly sleep-deprived self this semester and thank you for your positive affirmations regarding my progress in lab meetings every week.

Thank you to the amazing faculty I have had the pleasure of learning from and being inspired by at Mount Holyoke these past four years. In particular, I would like to thank Dr. Amy Camp for being in my corner as my advisor and committee member. You are an exceptional role model and I have cherished your support and advice these past few years. I would also like to thank my final committee member, Dr. Darren Hamilton for fostering my passion for organic chemistry and providing me with the foundation of knowledge that bolstered the work in this thesis.

A portion of this work was conducted by select members of the Ainslie Lab at the University of North Carolina Eshelman School of Pharmacy at Chapel Hill. In particular I'd like to acknowledge Cole Batty and Pamela Tiet for their contributions to the biological testing and applications of the materials I have developed in the Broaders Lab.

Finally, I'd like to thank my family for their infinite support of my academic career and their unconditional love from nearly three thousand miles away. Thank you for always being there to restore my confidence in myself after the many challenges presented in a journey like this.

Funding Acknowledgements

Broaders Lab:

Research conducted in the Broaders Lab was supported by the following sources: Mount Holyoke Fund the Future Award, Elaine Marieb Science Fund, and the National Science Foundation, Grant DMR 1808073

Ainslie Lab:

Research in the Ainselie Lab was supported by the National Cancer Institute of the National Institutes of Health under award number T32CA196589. This work was performed in part at the Chapel Hill Analytical and Nanofabrication Laboratory, CHANL, a member of the North Carolina Research Triangle Nanotechnology Network, RTNN, which is supported by the National Science Foundation, Grant ECCS-1542015, as part of the National Nanotechnology Coordinated Infrastructure, NNCI.

In memory of Dr. Elaine Marieb
1936-2018

Table of Contents

List of Figures

Abstract

Microparticulate immunotherapy holds promise to vaccinate against difficult targets like cancer. Many vehicles exist, but triggering is often based on pH or passive hydrolysis. The most effective cells at promoting an immune response are dendritic cells. The lysosomes of these cells are highly oxidizing relative to acidifying, so an oxidation-sensitive vehicle could be a significant advancement in this field. One promising class of materials being developed toward this end are aryl boronate-modified dextran polymers. Boronic esters for oxidation-sensitive delivery vehicles are typically made using pinacol (Pin) as a diol. However, Pin-based aryl boronate-modified polymers are prone to interchain transesterification that restricts their solubility and ability to be tuned and synthesized. This phenomenon also inhibits the polymers ability to be processed into discrete particles. To solve this, the diol used in the modified polymer was varied in order to develop a pattern for how the structural properties of different diols affect the behavior of the molecule as a whole. In addition to pinacol, (-)-pinanediol, norbornenediol, and cis-1,2-cyclopentanediol were tested using ^{1}H-NMR to track the formation and disappearance of key elements of interactions between their ester forms and dextran. The stability of these diols in other contexts have been assessed, but those conclusions have not yet been applied to the addition of those diols as boronic esters onto polymer backbones. It was confirmed that in accordance with patterns developed in literature, pinanediol formed the most stable boronic ester of the four analyzed and retained its stability when incorporated into a dextran polymer. This behavior is due to pinanediol's cyclic nature, rigidity, and high degree of steric hindrance.

Subsequently, the synthesis of a new aryl-boronate modified dextran polymer was achieved using pinanediol (PD) to replace Pin (PDB-Dex). This modified dextran improves upon Pin-based materials by maintaining its solubility in organic solvents and resulting in smooth, discrete, microparticles that are consistent in size. Microparticles were prepared and analyzed using SEM and DLS methods. Degradation of particles was triggered with hydrogen peroxide and tracked using ^{1}H-NMR to confirm the mechanism of degradation. A standard BCA Assay was adapted to measure the rate of degradation under physiologically relevant conditions, and it was found that PDB-Dex is sensitive to peroxide levels as low as 0.01 mM. Preliminary biological assays and in vitro studies show low cytotoxicity and the ability to deliver an immunostimulatory agent.

CHAPTER 1: INTRODUCTION

1.1: Drug Delivery

Drug delivery systems aim to improve the circulation and efficacy of their payloads in their host organisms through qualities like trigger-sensitivity and biocompatibility. This makes the field of drug delivery one that is interwoven with many others such as pharmacology, chemical biology, and organic chemistry. Drug delivery systems possess unique functional advantages that hold potential to outperform the basic use of medication alone for treatment of disease. They can be synthesized on the nano, micro, and macro scale. Vehicles on the nanoscale have been engineered to delay the dissemination of their payload in order to avoid non-specific uptake in undesired locations and target selected intracellular sites, a process generally known as passive targeting[1] Nanoparticles can also be modified with cell-specific ligands that facilitate active targeting.[2] Other materials have demonstrated the ability to pursue their targets *in vivo* through a network of mechanisms while bypassing the use of specific intracellular transporters.[3]

It is important to note that drug delivery is not to be confused with drug administration. They both can accomplish similar goals of treating a target area with an appropriate antidote, however, drug delivery focuses

on the manufacturing of vehicles that can navigate through an organismal system either independently or by direction of an outside force, while basic drug administration techniques expel a medication into the point of contact. Drug administration methods can be categorized in numerous ways such as the method of entry, the mechanism of action, or by a specific class of drugs to which they are compatible with.[4] When categorizing drug administration methods by means of contact with an organism, one typically notes routes such as oral, topical, ocular, intravenous, intramuscular, or subcutaneous. Each one of these techniques has both advantages and disadvantages, and consequently suits certain applications more than others.

A recent development in advanced drug delivery technology includes the use of wirelessly-controlled, subcutaneously embedded microchips to induce programmed release of drugs such as the human parathyroid hormone fragment used in treating osteoporosis.[5] The advantage of this method is its ability to control the daily dosage without the user's conscious effort to dose themselves. This advancement was inspired by the technology and concept behind pacemakers and initial clinical trials are promising.[6] The pitfalls however, include the limitation on how many doses can be loaded onto a chip and the range of drugs and corresponding conditions that can be treated.

Another contemporary development in drug delivery methods is the localized control of magnetic microbubbles via ultrasound-guided targeting.[7] These tunable and minimally invasive microbubbles (MagMB)

have demonstrated the ability to respond to magnetic and acoustic stimuli external to their environment *in vivo*. MagMB were prepared by attaching heparin-functionalized nanoparticles to protamine-functionalized microbubbles with the hope that protamine would eventually be displayed on the surface of the structures. MagMB were tested for acoustic destructibility and echogenicity as well as their biodistribution and pharmacokinetics *in vivo* in murine models and proved to be viable tools for targeted drug delivery under specific conditions. Ultrasound-triggered microbubble destruction has proven effective at releasing drug payloads, however low efficiency has limited this method's versatility.

These two examples are just a small sampling of innovative methods of controlled drug delivery that possess customizable formats and the capacity for site-specific targeting.[8,9] However, it is pertinent to note that both have limitations that can be overcome by looking towards other materials. The former is restricted by its carrying capacity and the latter has reported low performance in *vivo*.

The concept of engineering materials to target specific areas in an organism can be applied to techniques such as gene therapy chemotherapy, and immunotherapy.[10,11] It follows that a vehicle's payload can be genetic material, other molecules, or drugs.[12] This also implies that the vehicle itself can be either a soluble or particulate carrier. One area of drug delivery that has shown promise is particulate immunotherapy. This approach is useful because particles can be engineered to mimic the size of pathogens.

1.1.1: Particulate Immunotherapy

Particulate immunotherapy encompasses the concept of synthetically developed, biocompatible capsules that have the potential to encapsulate drug molecules to be distributed within an organism. The method of encapsulation and release is highly varied depending on the material and application. These vehicles are engineered to inherently respond to organismal environments, and many are tuned to react to a specific trigger condition, such as pH level, oxidation, or temperature.

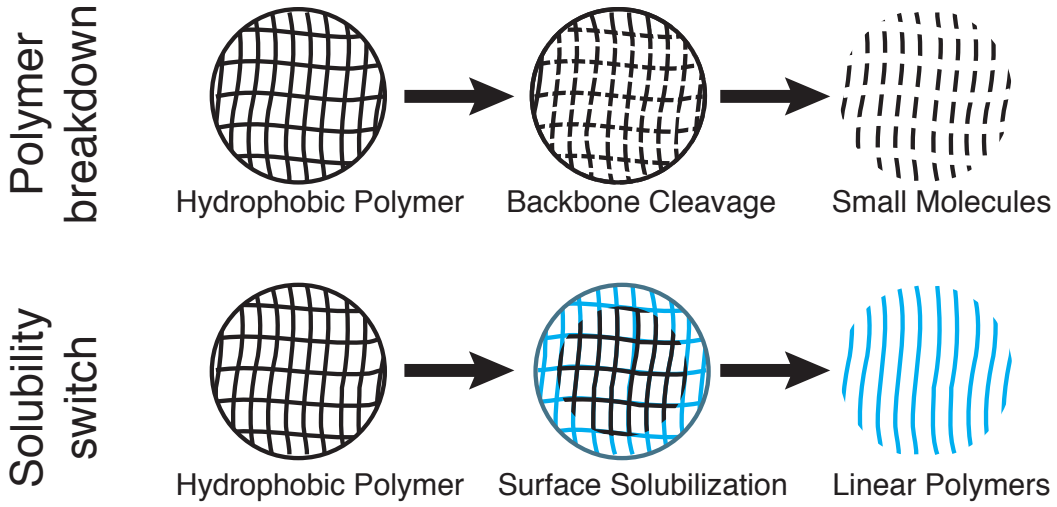

Figure 1. Solubility switching concept vs polymer breakdown. Polymer with hydrophobic properties breaks down via backbone cleavage and results in large concentrations of hydrophobic small molecules as byproducts. Polymer with dynamic properties can shift between hydrophobic and hydrophilic states.

The behavior of the material used for drug delivery as a function of its structure can be classified in several groups based on solubility properties. In order to maintain its structure after being processed into a capsule, the ability to resist immediate degradation is required. One such

method of achieving this capability is by using a hydrogel that regains solubility after hydrolysis of its crosslinks. A second concept is a hydrophobic polymer with a degradable backbone (**Figure 1**). Both of these types of materials are inherently water insoluble which makes them difficult to incorporate into an organismal system. A alternative option is a material that transforms its solubility properties upon triggering so that it is insoluble in its functional form and becomes soluble to release its contents. This concept of a solubility-switching, polymer-based particle has the potential to be more versatile than the aforementioned materials.

One effective way for drug delivery methods to have a direct impact on their host organism is to target components of the immune system. Incorporation of targeted delivery vehicles into the front line of defense against foreign pathogens has the potential to kick start and enhance immunological response by overcoming lysosomal barriers and reporting to specific tissues that are under "attack".

1.2: Immunology

Immunology is the study of the body's defense against infection. Current literature classifies virulent microorganisms (pathogens) into four categories: viruses, bacteria, fungi, and parasites.[13] Actions that organisms take in response to foreign pathogens are split into categories as well: innate immune response and adaptive immune response. As their names suggest, the innate immune response is readily available to fight pathogens that the body is already equipped to handle in a general sense,

while adaptive immune response reacts to specific pathogens and develops a lasting memory for them by inducing the production of antibodies, amongst other functions. Particulate immunotherapy materials interact primarily with the adaptive immune system. Additionally, they also can encapsulate drugs that affect the innate immune system.

The immune system is comprised of many specialized cells derived from bone marrow.[13] Depending on their role, the fates of each type of cell varies. Some reside in specific peripheral tissues and some circulate in the bloodstream or in the lymphatic system. One class of these cells is known as dendritic cells, named for their structure that includes protrusions that resemble the dendrites of nerve cells. Dendritic cells engulf external particles through phagocytosis and thus can degrade pathogens that they ingest. They also connect the innate and adaptive immune responses because they can activate T lymphocytes by presenting antigens derived from degraded pathogens on their surface. This ability qualifies them as antigen-presenting cells (APCs).[13]

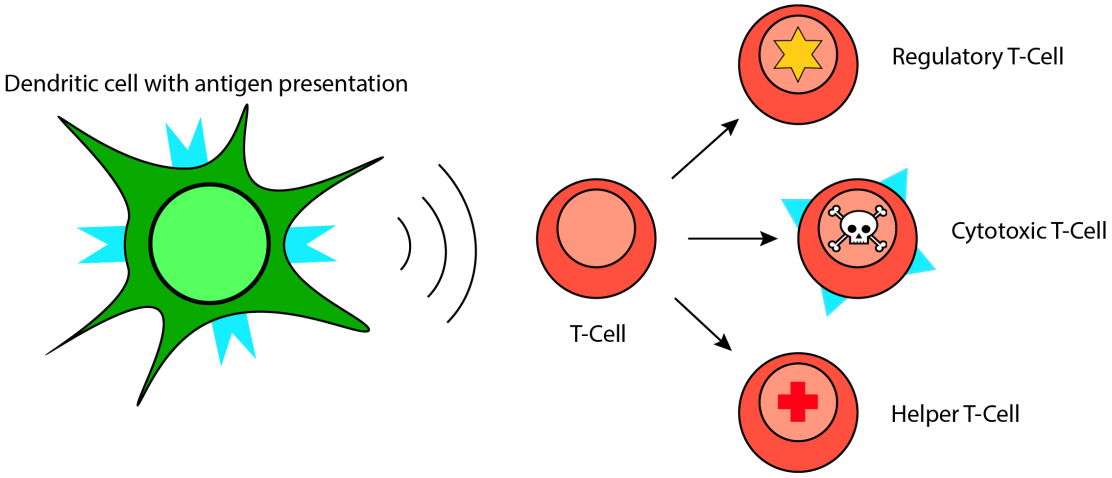

Figure 2. Dendritic cell signaling of T-cell differentiation. Dendritic cell (green) presents specific antigens (cyan) derived from a foreign pathogen and signals the differentiation of T-cells (red) through a series of steps. T-cells will then transform into one of the types shown.

There are two types of lymphocytes: T lymphocytes (T cells) and B lymphocytes (B cells).[13] Both types of cells have a mechanism of action that requires antigen-specific activation and involves subsequent proliferation and differentiation of the original cell. When T cells are activated by an antigen it can differentiate into one of three classes of effector T lymphocytes: killing, activation, and regulation (**Figure 2**). Cytotoxic T cells kill infected cells, helper T cells assist in directing the behavior of other cells through organized signals, and regulatory T cells suppress the activity of other lymphocytes for additional control of the immune response.[13] When an antigen binds to a B-cell receptor on the surface of a B-cell, the cell multiplies and differentiates into plasma cells. Plasma cells produce antibodies, which are mobile forms of the B-cell receptors that then target the same antigen that originally bound to the B-cell. T cells and B cells are key components of the adaptive immune

response and targets of microparticle manipulation because of their gateway-like roles in triggering immune response.

1.3: Microparticulate Immunotherapy and Immunology

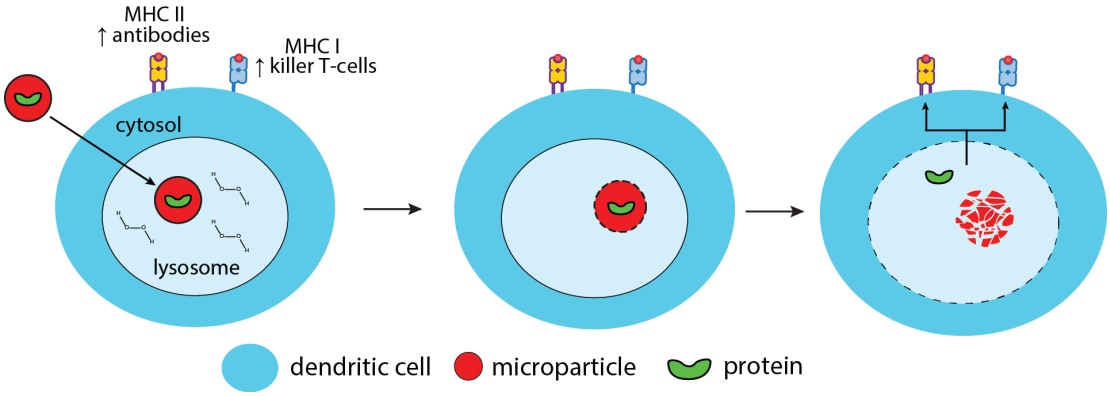

Figure 3. Mode of action of a degradable microparticle inside a dendritic cell. A protein loaded microparticle passes through dendritic cell membrane and degrades upon oxidation, triggering lysosomal degradation. Previously encapsulated protein is then released into the cytosol to interact with MHC I and MHC II downstream in the immune system.

Immunotherapy relies on the delivery of antigens to antigen presenting cells. Microparticles that are designed to degrade upon specific trigger conditions within cells can customize the speed or locations at which the processes of the adaptive immune system occur. Initially, APC's engulf the particles, creating an endosome. The endosome matures into a lysosome, where the particles are exposed to certain conditions such as increased reactive oxygen species (ROS) levels or low pH. When the appropriate environmental conditions are met, the particle is triggered to degrade and ruptures, releasing its payload into the lysosome (**Figure 3**). Additionally, it is theorized that the degradation of microparticles causes

the disruption of the lysosomal membrane though an osmotic mechanism.[14] This occurs when water rushes to surround each degraded component of the particles and encapsulated material. Consequently, the overall solute concentration of the lysosome increases rapidly, which forces water in, down the concentration gradient, in efforts to balance relative osmolarity between the cytosol and the lysosome. At this point, it is suggested that entire lysosome lyses, releasing the contents of the particle and its byproducts of degradation into the cytosol.

In order to incorporate delivery vehicles as a segue into the immune system, they have to encapsulate a moiety that can interact with key components of the adaptive immune response. Previous work has produced such a particle that is triggered by low pH levels and successfully encapsulated ovalbumin (OVA), which can elicit presentation on major histocompatibility complex class I (MHC I) and MHC II.[3] MHC I presents peptides derived from the cytosol and eventually leads to killer T-cell activation. MHC II presents peptides derived from lysosomal proteins and kickstarts antibody production. MHC I can also present lysosome-derived peptides, a concept known as cross-presentation.

1.4: Oxidation

Oxidation, simply put, is the loss of electrons. This phenomenon plays a significant role in many aspects of biological regulation and chemical synthesis. Oxidation is almost always coupled to the concept of reduction in oxidation-reduction reactions, or redox reactions (**Figure 4**).

Redox reactions are processes in which a flow of electrons occurs. A prominent example of the application of redox reactions with vital biological relevance is their role in glycolysis and the citric acid cycle and more specifically, oxidative phosphorylation. The energy released by redox reactions is used to fuel the performance of unfavorable processes, namely the formation of adenosine triphosphate (ATP). That redox-derived energy is used to power a proton pump that creates a gradient across the mitochondrial membrane. While this may be the most commonly referenced role of oxidation in biology, there are countless other phenomena occurring simultaneously that utilize the same principles of electron transfer.

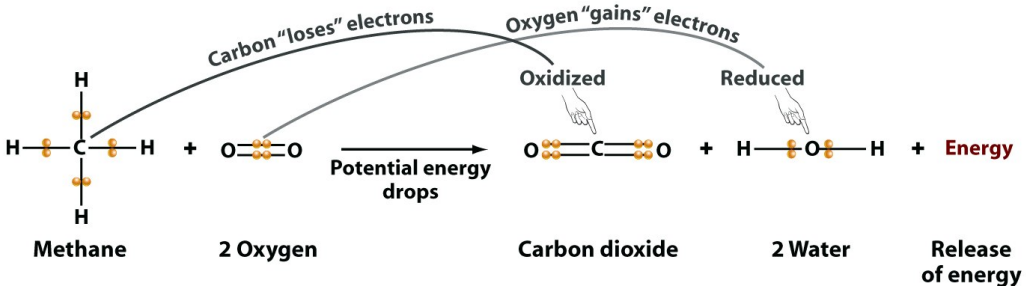

Figure 4. Combustion of methane, an oxidation reduction reaction[15]

The process of aerobic metabolism generates ROS, which build up in the body and are usually balanced by cellular antioxidants. ROS can be involved in cellular stress, signaling, defense and many other aspects of cellular functions.[16,17] If they are not balanced, they can cause the degradation of nucleic acids, proteins, and lipids in a condition called oxidative stress.[16] Oxidative stress can be a threat when it is not controlled, but it is also an effective way to trigger the immune system.[18] A process

called oxidative burst occurs in mammals to combat invading microorganisms with ROS-releasing neutrophils. Lysosomes also utilize oxidation when interacting with APC's and targeting foreign pathogens for destruction.[17] Previously, microparticle degradation within the lysosome was prompted by pH changes like acidity, but it has been shown that dendritic cells have more ROS and a higher pH than macrophages, so the use of oxidation rather than acidity as a trigger could be more effective[19].

Due to its prevalence in living organisms, oxidation has been highlighted as an effective means of triggering physical changes to the chemical structure of biocompatible polymers. For example, crosslinked poly(propylene sulfide) has been used in the design of nanoparticles that execute the release of hydrophobic drugs upon oxidation to poly(sulfone).[20] This transition from sulfide to sulfone leads to a large change in hydrophobicity, and leads to particle swelling and cargo release.

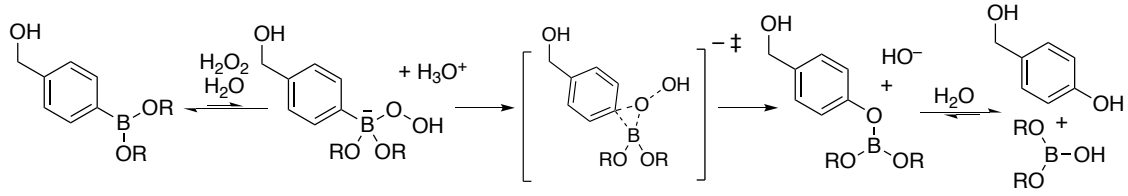

Scheme 1. Mechanism of H_2O_2-mediated oxidation of phenylboronic acid to phenol

Recently, boronic esters have become more prevalent as oxidation-responsive elements in molecular sensors and drug delivery vehicles.[8] Oxidation reactions involving boronic acids serve as a basis for a more complex degradation mechanism. When exposed to H_2O_2, arylboronic

esters and acids are transformed to phenols through a mechanism involving peroxide association, insertion into the C–B bond, and hydrolysis (**Scheme 1**)**.** When part of a larger molecule, this simple oxidation is a singular, but central, component of the breakdown of the entire moiety, that could potentially contain a wide variety of modifications.

1.5: Boronic Acids and Boronic Esters

Boronic acids are a class of compounds derived from boric acid, $B(OH)_3$, where one of the three hydroxyl groups has been replaced with an alkyl or aryl group. Boric acid itself is known to be very stable and well tolerated by humans, however, derivations of its structure do not necessarily share all of the same qualities.[21] Structural differences of varying degrees can cause shifts in behavior in certain environments which is what makes certain derivatives suitable for drug delivery, and some not. Boronic acids most commonly form esters through an equilibrium reaction in which the forward reaction is highly favorable under specific conditions.[22] Boronic acids, unlike carboxylic acids, are not found in nature, but their reactivity as mild Lewis acids, and their stability make them attractive options for larger molecule modification.[23]

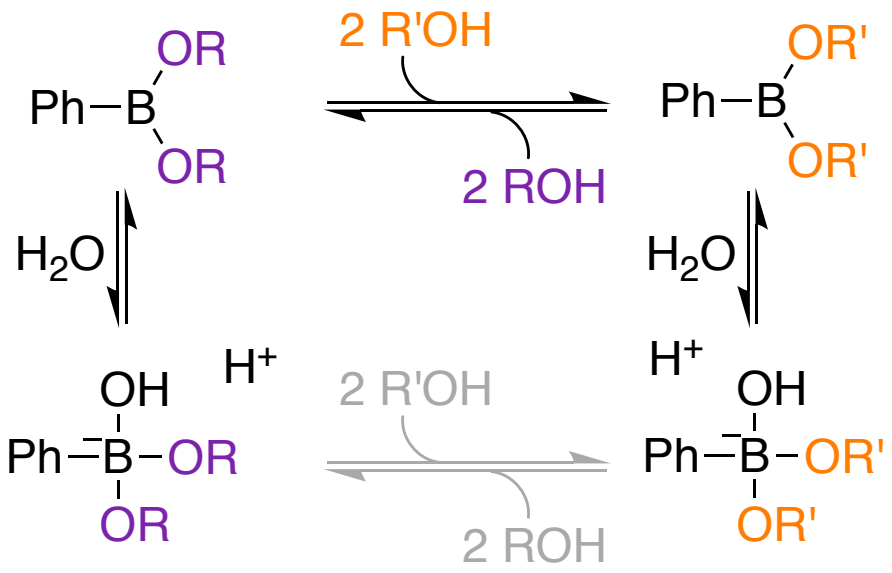

Scheme 2. Transesterification of boronic esters. Reaction proceeds first via addition to boron in its trigonal sp^2 form, rather than dissociation from boron in its tetrahedral sp^3 form. R = alkyl or H

A unique and useful quality of boronic acids is that they exist as an equilibrium of their trigonal planar and tetrahedral forms (**Scheme 2**). This property allows for an exchange reaction to happen through an associative mechanism. More specifically, it proceeds as an addition-elimination as opposed to an elimination-addition. Boronate esters, also known as boronic esters, (or simply boronates) are formed through the replacement of boronic acids' hydroxyl groups with alkyl or aryl ethers. This transformation renders boronic esters less polar due to the loss of the hydroxyl group, which lent hydrogen bond donor capabilities to the moiety.[23] This reaction is reversible and typically fast when performed with preorganized diols and when the product is insoluble in the reaction solvent.[23] The compounds focused on in this study were primarily boronic esters formed by the combination of boronic acid and a diol derived from a

cyclic ring. Rigid, 6-membered, cyclic diols tend to be the most resilient boronic esters toward hydrolysis and transesterification.[23] It is postulated that this is the case because the geometric organization of boron in relation to its adjacent lone pair-adorned oxygens is more favorable in rings with more than 5 members.[23]

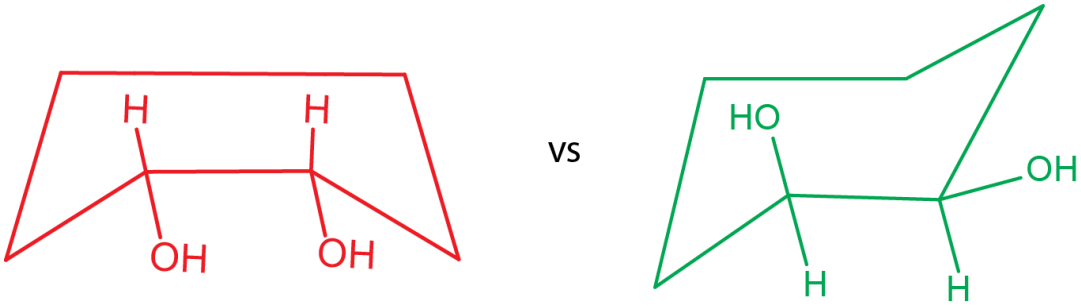

Figure 5. Restricted vs relaxed chair conformer of *cis*-cyclohexane-1,2-diol. Red indicates less favorable conformer and green indicates more favorable.

Structural distinctions between various diols contribute to the relative ease of boronic ester synthesis, and stability of the resulting product. For example, early studies into the effect of diol structure on boronic ester synthesis came to the conclusion that the location of the two hydroxyl groups in relation to each other causes puckering in cyclic diols.[24] More specifically, when all the carbon-oxygen bonds are in the same plane, as in the case of *cis*-cyclohexane-1, 2-diol, the result is an unstable boat confirmation and ester synthesis is inhibited. Contrastingly, when one hydroxyl group is equatorial, and one is axial, the molecule is more stable and ester synthesis is favorable (**Figure 5**).[24] This case is a prime example of the importance of sterics in vicinal diol behavior and consequently, boronic ester behavior.

The relative stability of combinations of boronic acids and diols has been studied for the purposes of kinetically and thermodynamically evaluating the biorthogonal conjugation reaction that ensures tight boronate formation.[25] The structure of both diols and boronic acid derivatives, with particular attention to constituent placement, has been shown to have distinct effects on the kinetics of these reactions. In this study, the behavior of various boronic acids was the primary concern. Their results highlight the importance of chemical structure in relation to the hydrolytic stability of boronic esters with boronic acids as contributing factors. It was found that isopropyl groups as substituents on boronic acids improved stability, while halogens and other electron withdrawing groups in general, decreased stability. These structural and compositional differences were mainly highlighted in the acid components of boronic esters, however with many of them being common functional groups in both diols and boronic acids, it is likely that many of the same principles can be applied to the behavior of boronic esters based solely on diol variation.

1.6: Dextran

Dextran is a polysaccharide primarily consisting of α-1,6 glycosidic linkages between glucose monomers (**Figure 6**). Its branches are connected through α-1,3 linkages. The degree of branching in any given unit of polymer varies based on factors such as the species of bacteria that

created it, the temperature it was synthesized at, and the concentration of the materials provided to the bacteria to synthesize it.[26] The dextran used in this study contained less than 5% branching. Dextran chains can vary in molecular weight, anywhere from 3 to 2,000 kDa. Dextran is synthesized from sucrose by bacteria such as Leuconostoc.[27] Dextran has a plethora of uses in medicine, because it is generally safely compatible with the human body and with other organisms.[28] It is used to combat hypovolemia during surgery and to treat postoperative venous thrombosis. Dextran's plasma half-life can be as short as 2 hours, a useful time range for a component of a drug-delivery system.[29]

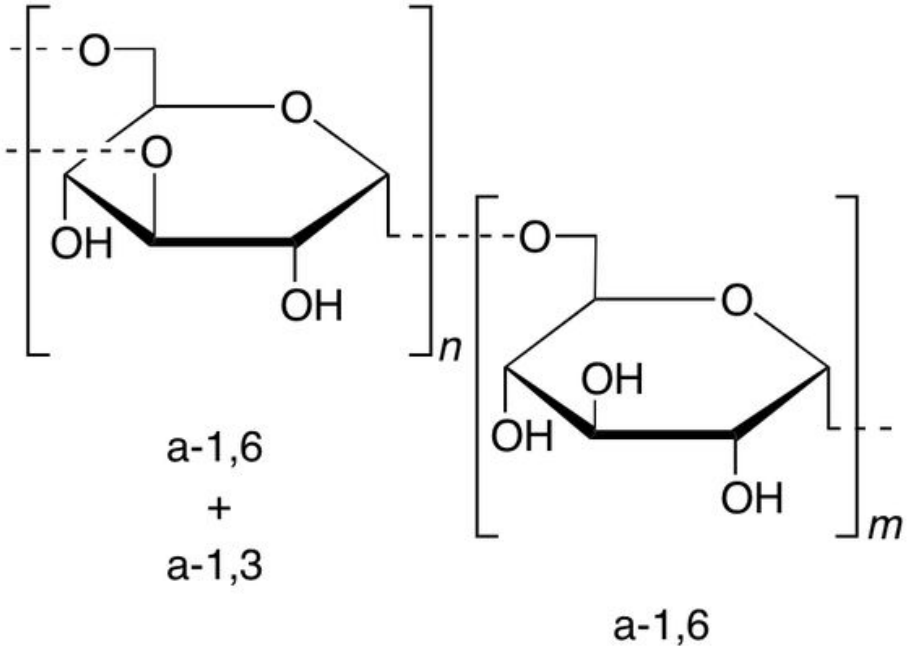

Figure 6. Chemical Structure of dextran (~10K = 66-67 AGUs)

The ability of specific small-molecule modifications to alter the solubility of pure dextran is in part, due to dextran's inherent structure and properties. Dextran has already proven to be a viable backbone for

pH-sensitive polymer-based microparticles.[3] The formation of various acetals linking adjacent hydroxyl groups of single glucose units changes dextran's solubility properties. When hydrolysis is catalyzed by acidic conditions the polymer degrades. This causes the particle to release its encapsulated payload, and the byproducts of that process primarily include water-soluble, unmodified dextran. Only a small number of polymers are soluble in both water and water-miscible organic solvents, which narrows the possible materials eligible for modification in the ways that dextran can be altered.

Dextran is also a preferred base for synthesizing biocompatible hydrogels.[30] Hydrogels are three-dimensional hydrophilic complexes of polymers that can absorb large amounts of water. They have also been shown to have drug delivery capabilities. Hydrogels synthesized from methacrylated dextran (dex-MA) and lactate hydroxyethyl methacrylate-derivatized dextran (dex-lactate-HEMA) were evaluated for biocompatibility. Dex-MA, a nondegradable material showed no toxic effects on surrounding tissues, and dex-lactate-HEMA, a degradable hydrogel, did not produce toxic byproducts once degraded *in vitro*.

1.7: Prior Art and Project Goals

The work presented in this thesis builds off of a previously published material known as Oxi-Dex (and from here on will be referred to as PinB-Dex).[31] PinB-Dex is an oxidation-sensitive, biocompatible polymer with a dextran backbone that was modified with pinacol boronic

ester. Its invention highlighted the benefit of using oxidation rather than pH as a triggering mechanism for particulate immunotherapeutic materials. However, it suffered from poor solubility and processing issues, rendering it unsuitable for further exploration as a potential drug delivering material.

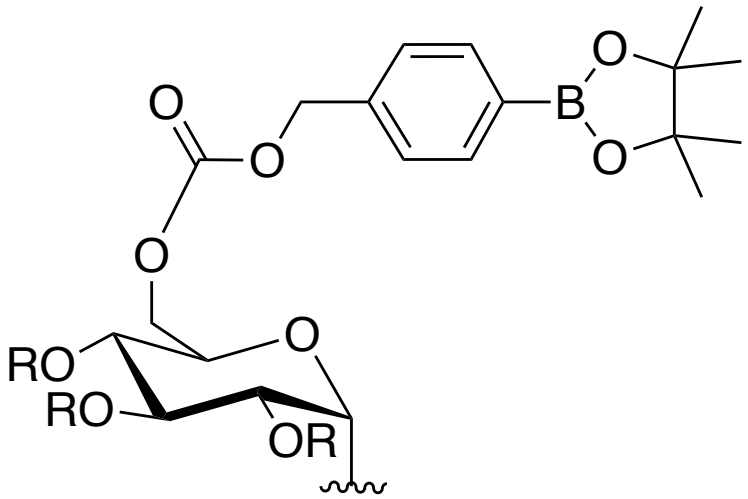

Figure 7. Structure of PinB-Dex. ~~~ represents repeating anhydroglucose units

The following study combines organic synthesis protocols and materials chemistry to accomplish two main objectives. The first is to explore the class of diols that have been referenced or tested in previous work with varying contexts and develop a pattern of behavior based on structural and compositional nuances between diols. This pattern could be useful in predicting diols that would be the most suitable components for arylboronate modifications to polymers like dextran. With that pattern established, the second objective of this work is to engineer a dextran based, biocompatible polymer that can be easily synthesized, effectively used in a biological setting, and whose degradation is triggered in

oxidative conditions. Pinacol, the diol used in PinB-Dex, did not contribute adequately to the stability of the ester it formed, and thus created processing issues that rendered PinB-Dex difficult to work with and inefficient. It was postulated that using a cyclic, rigid, more sterically hindered diol could improve the stability of the boronate modifications, and thus enhance the specialized polymer's characteristics and functionality.

CHAPTER 2: VARYING DIOLS IN BORONIC ESTERS

2.1: Theory

The concept of modifying hydroxyl groups on glucose units in dextran is an underexplored method of altering dextran's chemical properties. Boronic esters are a useful choice for these modifications, and their diol elements are essential components of their composition. Additionally, boronic acids are divalent, requiring two constituents to achieve stability, thus supporting the use of diols as esterifying agents. However, the degree of ease through which those modifications are implemented and sustained varies with both the diol identity and the acid identity.

A diol is defined as a compound with two hydroxyl groups in its structure. With that simple parameter in mind, the variation in total structure and composition of diols in general is wide. It includes molecules as simple as ethylene glycol, one of the most common diols, to (*S*)-2,2′-Diphenyl-4,4'-biphenanthrol, commercially known as Vapol, used primarily as a ligand in Diels-Alder, imine aldol, and azidirination reactions.[32–34] (**Figure 8**).

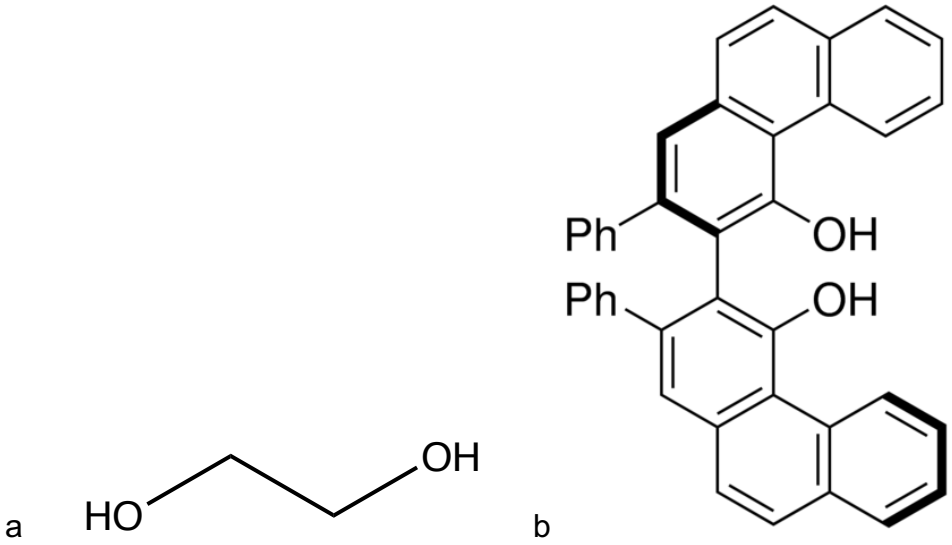

Figure 8. Structures of a. Ethylene Glycol and b. Vapol

There are several main subcategories of diols that indicate the bond separation between the two hydroxyl groups. Geminal diols have hydroxyl groups that are bonded to the same atom and are prepared through hydration of aldehydes and ketones. The hydration reaction is typically unfavorable except in a few cases such as the hydration of formaldehyde to methanediol. Diols exist in equilibrium with their hydration products when in water, and the unfavorable reactions tend to favor the starting materials. A second group of diols are vicinal diols (also known as glycols), which have hydroxyls on adjacent atoms. The creation of glycols can be completed through the hydrolysis of epoxides or through the oxidation of an alkene. A third class of diols are 1,3-diols, often prepared through aldol condensation of ketones with formaldehyde and then catalytic hydrogenation of the resulting carbonyl. Llonger diols are less common

and can be prepared by hydrogenation of diesters of various carboxylic acids.

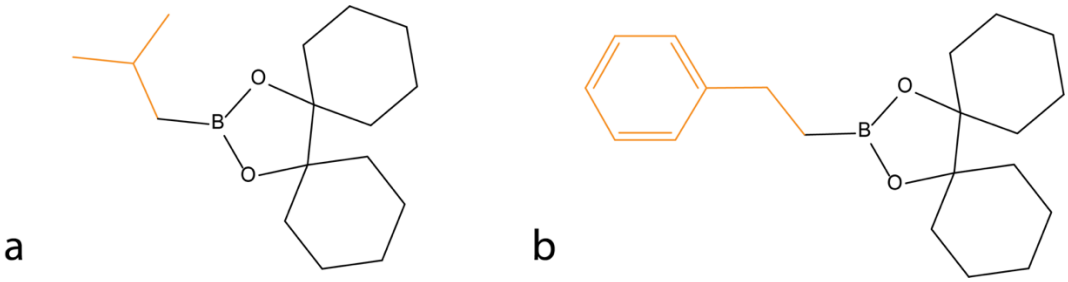

Figure 9. (1,1'-bicyclohexyl)-1,1'-diol esters. a) isobutylboronic ester and b) 2-phenylethylboronic ester

The diols used in this study are all cyclic vicinal diols that can esterify with arylboronic acids. It has been shown that hindered, pre-organized, vicinal diols alleviate the entropy loss that occurs during boronic ester formation, and therefore create the most tightly bound boronic esters.[36] The notion of boronate stability increasing with steric hindrance was further explored and confirmed using variants such as (1,1'-bicyclohexyl)-1,1'-diol and assessing rates of hydrolysis. (1,1'-bicyclohexyl)-1,1'-diol esterified with isobutylboronic acid was stable for up to 60 hours with no hydrolysis and when esterified with 2-phenylethylboronic acid and inspection by both ^{1}H-NMR and HPLC, showed comparable stability to the same acid with pinanediol (**Figure 9**).[37] It is also known that pH effects the affinity of diols and boronic acids for each other, and it has been shown that the K_{eq} of the esterification of phenylboronic acid with diols increases with higher pH.[38] The effect of pH on boronic ester stability is

key because hydrolytic stability at physiological pH is a principle aim of the material in its final polymeric form.

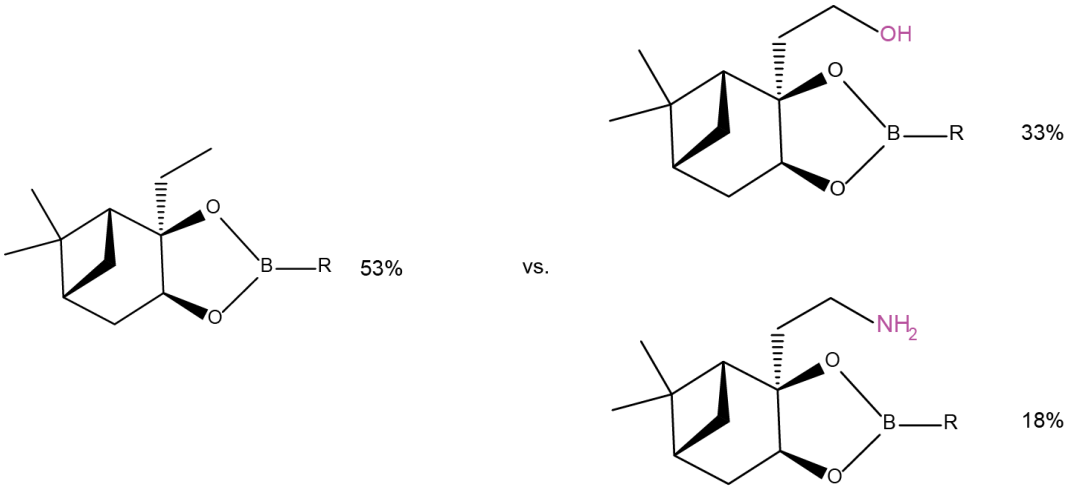

Figure 10. Relative rates of formation between diols with and without coordinating or chelating groups. Adapted from Roy and Brown.[39] The addition of a hydroxyl group (coordinating) or an amine group (chelating) does not increase the rate of formation via transesterification from pinanediol boronic ester as much as a similarly structured diol does without such groups.

Other notable properties of diols that are hydrolytically stable are ring size and the identity of the constituent on the hydroxyl-bearing carbon. 6-membered cyclic diols are more stable than their 5-membered analogs when esterified with phenylboronic acid.[40] Curiously, the addition of coordinating or chelating sites to the hydroxyl-bearing carbon by means of a short alkyl chain does not seem to increase stability or favorability in esterification when compared to unmodified alkyl chains without such sites (**Figure 10**).[39] Increasing steric bulk specifically around one of the hydroxyl-bearing carbons tends to increase stability as well (**Figure 11**).

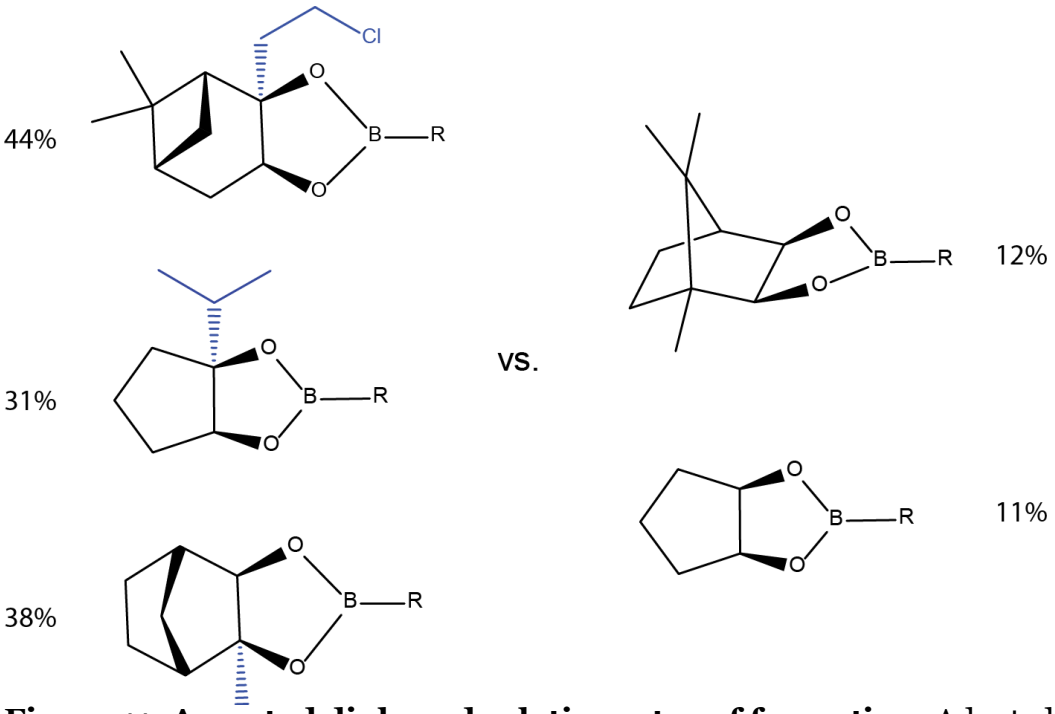

Figure 11. Assorted diols and relative rates of formation. Adapted from Roy and Brown.[39] The diols above were synthesized via transesterification from pinanediol in its ester form with methylboronic acid. Diols that included substituents on one of the hydroxyl-bearing carbons, and thus added steric hindrance, had consistently higher rates of formation. Substituents are highlighted in blue.

As for the behavior of boronic acids, the empty p-orbital of boron renders them susceptible to interactions with electron-donating atoms. It has thus been postulated that boronic esters could be stabilized through interactions with electron donors, reducing their vulnerability to nucleophilic attack.[37] Additionally, it has been shown that *ortho*-methyl and isopropyl substituents on the acid improved stability, likely due to bulkiness. It was also found that halogens and other electron-withdrawing groups on the acids decreased stability which corresponds to the finding that hydrolytic stability was linearly correlated with acidity in arylboronic acids.[25]

2.2: Results and Discussion

2.2.1: Pinacol vs Pinanediol with a Dextran Excess (A)

With the desired structural parameters highlighted above in mind, we predicted that (-)- pinanediol (which will from now on be referred to simply as pinanediol or PD) would perform the most efficiently when reacted with 4-(hydroxymethyl)phenylboronic acid.

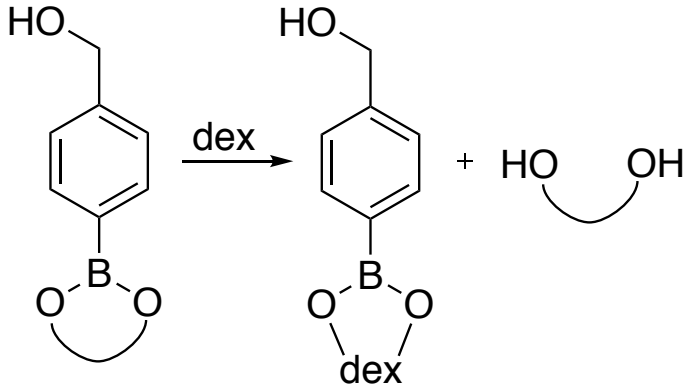

Scheme 3. Transesterification between 4-(hydroxymethyl)phenylboronic acid and a cyclic diol. Hypothesized interaction between pinacol boronic ester and dextran resulting in the replacement of pinacol with dextran as the "diol" component of the ester. Pure pinacol is then cleaved from the acid and remains in solution in its pure diol form.

A direct comparison of the interaction between PD boronate or pinacol boronate and an excess of dextran monitored via ^{1}H- NMR spectroscopy shows that pinanediol forms a boronic ester that is not prone to transesterification with dextran, while pinacol shows signs of instability. This can be seen specifically in the transition from the pure form of both diols to their respective boronates and their behavior when exposed to dextran.

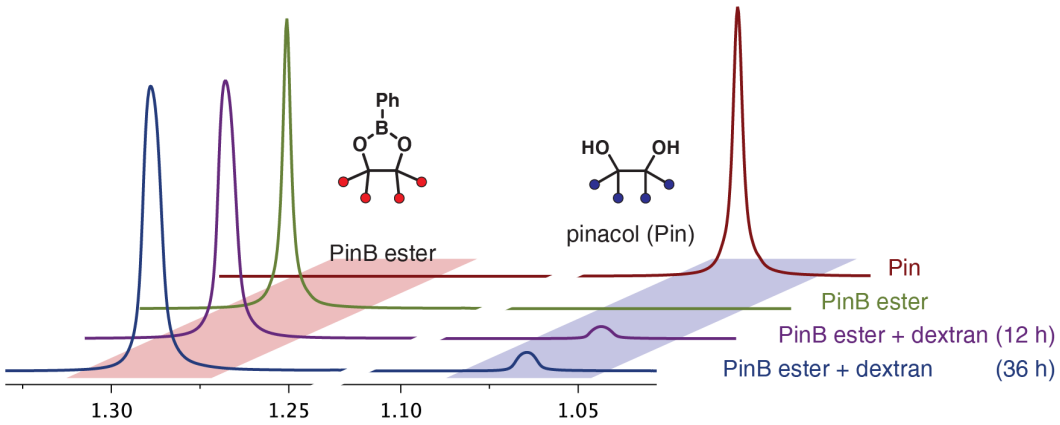

Figure 12. Relative stability of PinB ester when combined with dextran ^{1}H-NMR monitoring shows that after 12 and 36 hours, pure pinacol appears in solution.

The spectra show that when pinacol is esterified and combined with roughly a 3.5 molar excess of dextran, there is a fraction of the pure form of pinacol (1.05 ppm) that reappears in solution after disappearing during the initial esterification (**Figure 12**). That phenomenon does not occur with pinanediol which is supported by the evidence of distinct sets of peaks for each moiety and the persistence of the same peaks through 36 hours (**Figure 13**). Comparing integrations of those latent peaks against control peaks that occur in all spectra allowed for the conclusion that with an excess of dextran, 6.2% of pinacol in the solution transesterified in 36 hours. Based on the amount of dextran in the solution and assuming that each branch can bind a single boronic ester, a maximum of 17.5% of the pinacol in solution could have potentially transesterified. It follows then, that 36% of *possible* transesterification reactions actually occurred. This particular transesterification phenomenon is one that hinders the

formation of the functional, oxidizable PinB-Dex and will be covered in more detail in the next chapter.

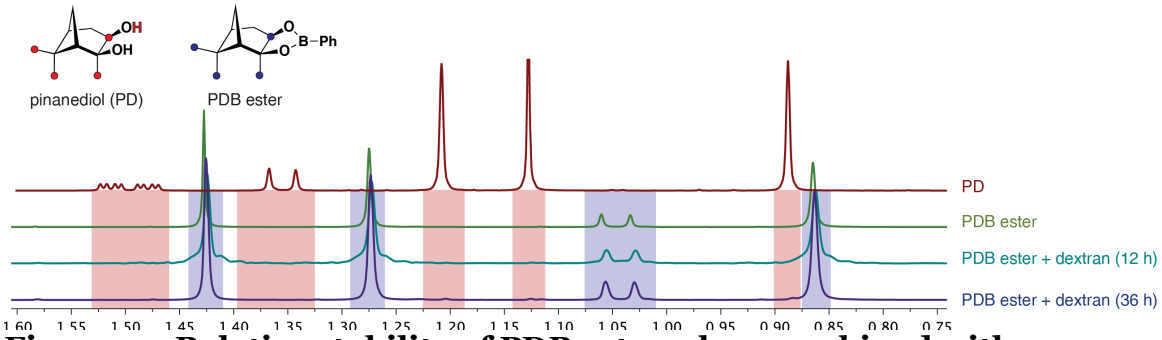

Figure 13. Relative stability of PDB ester when combined with dextran. Pure pinanediol does not appear in solution after 12 and 36 hours.

2.2.2: Pin vs PD with a Dextran Excess Second Trial (B)

To replicate and confirm the results of the previous experiment, new samples of pinacol boronate and pinane boronate were synthesized and combined with dextran in an NMR tube. ^{1}H-NMR spectra were collected for the same amount of time (**Figure 14b**). Pinanediol continued to show no signs of instability and pinacol showed increased instability, prompting 11.7% transesterification before 36 hours. The peaks used in this measurement are shown in **Figure 16a**. This increase in transesterification could be explained by the larger ratio between pinacol and the excess of dextran added to the solution. The ratio of dextran to pinacol was increased to a 4.5 molar excess for this experiment, which could explain the change in degree of transesterification.

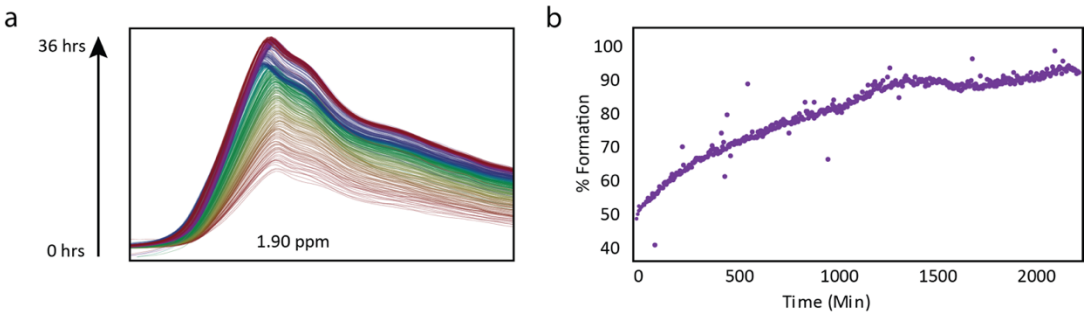

Figure 14. Appearance of pure pinacol over time. a.^{1}H-NMR peak indicating the reappearance of pure pinacol in 36 hours in a solution originally composed of its ester form and dextran. This reappearance was used to measure the degree of instability of pinacol boronate when attached to dextran. b. Percent formation of pinacol over time as a ratio of each peak integration compared to the final peak integration. Data was obtained from a standard proton NMR with scans collecting at a consistent speed over 36 hours.

2.2.3: Cis-1,2-cyclopentane and Norbornene Test (C)

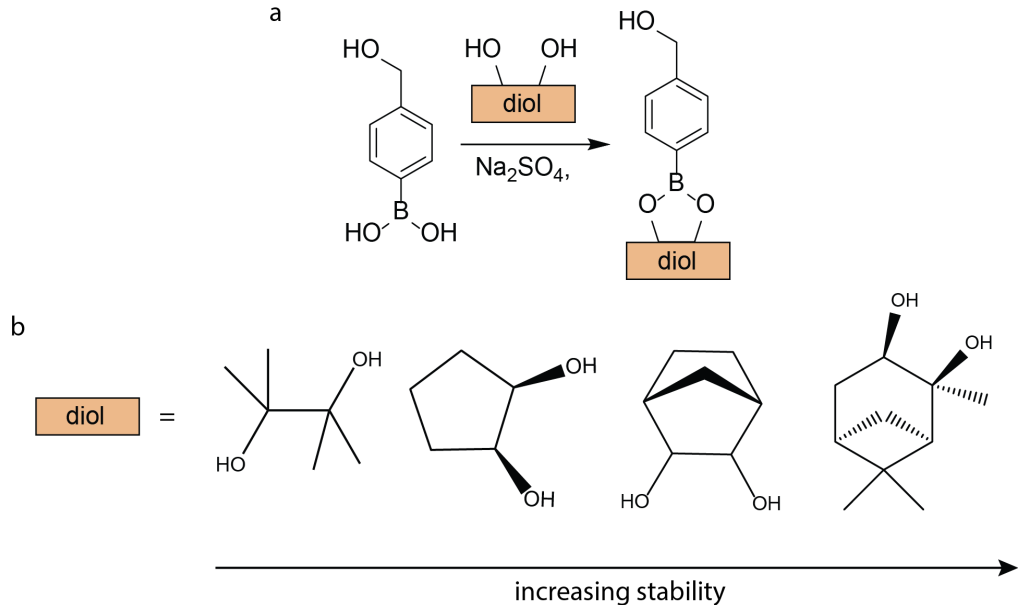

Figure 15. General boronic ester formation and diols tested in this study. a. Scheme of general boronic ester formation using a single diol that esterifies with both hydroxyl groups. b. Diols used in the study in increasing order of predicted and confirmed stability. From left to right: pinacol, cis-1,2-cyclopentanediol, norbornenediol, (-)-pinanediol.

To further explore the predicted trend of diol stability in the context of arylboronate modified dextran, *cis*-1,2-cyclopentane boronate (from here on referred to as cyclopentane boronate) and norbornene boronate were studied (**Figure 15b**). A similar ^{1}H-NMR experiment was performed to monitor the degree of transesterification that occurred when either of these diols were used as esters in concert with dextran. However, this time instead of using an excess of dextran, a stoichiometric equivalent of dextran was used to reduce the overall concentration of the samples. This allowed for clearer signals as polymer peaks in NMR are often difficult to interpret. The peaks ultimately used for analysis can be found in **Figure 16b,c**. It was found that in 21 hours, cyclopentane boronate resulted in 2.7% transesterification and norbornene boronate resulted in 1.5% in the same amount of time.

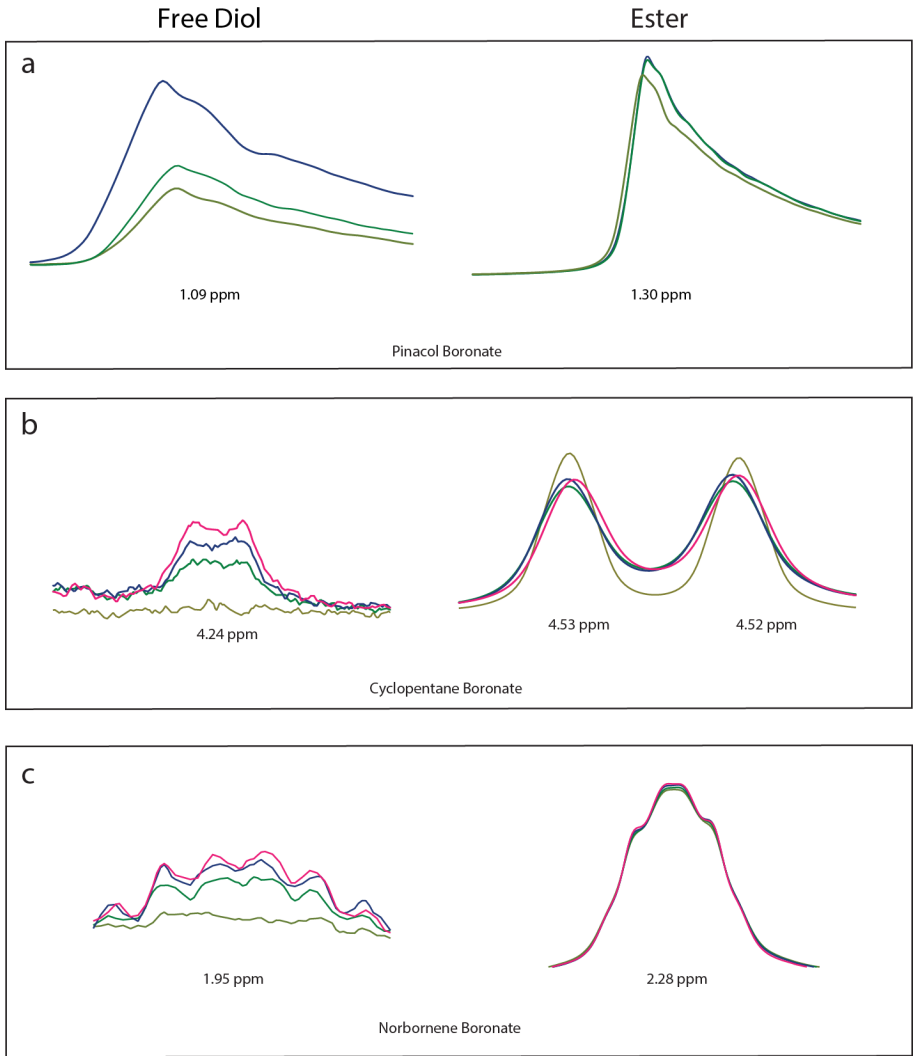

Figure 16. ^{1}H-NMR Peaks used for quantification of transesterification. a. Peak used to quantify transesterification of pinacol boronate and dextran complex (left) was compared to a peak with consistent signal as a control to obtain a ratio (right). b. Peak used to quantify transesterification of cyclopentane boronate and dextran complex (left) was compared to a peak with consistent signal as a control to obtain a ratio (right). c. Peak used to quantify transesterification of norbornene boronate and dextran complex (left) was compared to a peak with consistent signal as a control to obtain a ratio (right). For all parts, olive green represents the t=0 hr time point, kelly green is t=3, blue is t=21 and pink is t=77.

2.2.4: Summary of Diol Instability

The diols in this study were chosen based on their topology, rigidity, and degree of steric hindrance (**Figure 15**). Ultimately it can be concluded that pinacol lead to 6.2% transesterification, cis-1,2-cyclopentanediol lead to 2.7%, norbornenediol lead to 1.5%, and pinanediol showed no evidence of function-inhibiting transesterification (**Figure 17**). This outcome reflects the trends shown in the literature in that pinacol is the only non-cyclic, non-rigid, least sterically hindered diol used, and those qualities lead to its instability in boronic ester form. *Cis*-1,2-cyclopentanediol is cyclic and rigid, but is the least sterically hindered out of the 3 cyclic, rigid diols used in the study, which explains its place as the second-most underperforming diol. Norbornenediol is slightly more sterically hindered than cis-1,2-cyclopentanediol, which merits its place in the hierarchy. Finally, pinanediol performed the best, as it resisted transitioning out of its boronic ester form, and therefore the polymerized dextran complex was not vulnerable to transesterification at all.

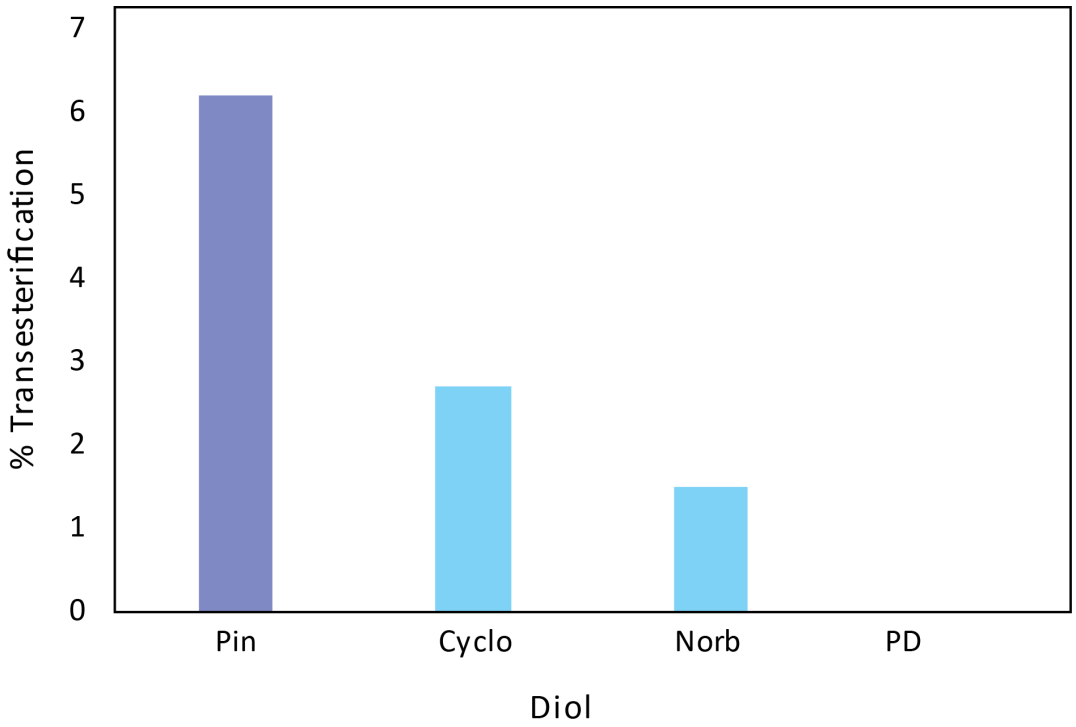

Figure 17. Summary of percent transesterification of all diols tested. Pin= pinacol, cyclo=cyclopentanediol, norb=norbornenediol, PD=pinanediol. Pinacol data taken from **A,** cyclo and norb data taken from **C**, PD data confirmed in both **A** and **B**. Pinanediol shown in lilac to indicate that its value was obtained using a 3.5 molar excess of dextran while others were not.

2.3: Methods

Synthesis of Pinacol boronic ester (PinB Ester) (A)

Pinacol (2.91 g, 24.6 mmol) was combined with phenylboronic acid (1.00 g, 8.20 mmol) in tetrahydrofuran (THF, 10 mL). Reaction was mixed on a rotisserie overnight and dried over sodium sulfate. The solution was concentrated under vacuum and dissolved in ethyl acetate (20-40 mL) and washed with water (3 x 10 mL) and brine (10 mL). 1H NMR (400 MHz, DMSO-d6) δ 7.73 – 7.64 (m, 1H), 7.54 – 7.46 (m, 0H), 7.41 – 7.34 (m, 1H), 1.30 (s, 6H).

Pinanediol boronic ester (PDB Ester) (A)

The same procedure as above was repeated with the replacement of pinacol with pinanediol (1.40 g, 8.20 mmol). A dry column vacuum chromatography (DCVC) column was run on the product in a gradient elution from hexanes to ethyl acetate. Rf = 0.385 in 3:1 hexanes and ethyl acetate. 1H NMR (400 MHz, Chloroform-d) δ 7.89 – 7.77 (m, 1H), 7.54 – 7.44 (m, 1H), 7.43 – 7.36 (m, 1H), 4.48 (dd, J = 8.8, 1.9 Hz, 1H), 2.49 – 2.40 (m, 1H), 2.25 (ddd, J = 10.8, 6.1, 2.2 Hz, 1H), 2.18 (dd, J = 6.1, 5.0 Hz, 1H), 2.04 – 1.94 (m, 1H), 1.51 (s, 2H), 1.34 (s, 2H), 1.25 (d, J = 10.8 Hz, 1H), 0.92 (s, 1H).

Measurement of transesterification of boronic esters by NMR (A)

PinB Ester and PDB Ester were dissolved in deuterated dimethyl sulfoxide and standard proton NMR spectra were collected. Spectra for pure pinanediol and pinacol were also collected as controls. Subsequently, PinB ester or PDB Ester was combined with dextran (50 mg/mL) in d-DMSO and time-lapse spectra were collected for 12 and 36 hours.

Synthesis of Pinane Boronate (B)

Pinanediol (4.83 g, 28.37 mmol) and 4-(hydroxymethyl)phenylboronic acid (4.31 g, 28.37 mmol) were stirred overnight with sodium sulfate (~8 g) in THF (45 mL). Heterogenous solution was filtered via vacuum to separate sodium sulfate from finished product. The filtered solution was then concentrated in vacuo and also under high vacuum to obtain a thick

clear oil on the verge of solidifying spontaneously. The sample was then purified using dry column vacuum chromatography (DCVC) using a gradient elution from hexanes to ethyl acetate. Product formed a thick pale yellow oil. Rf = 0.385 in 3:1 hexanes and ethyl acetate. Fractions were combined and concentrated *in vacuo* to a pale yellow oil (7.6 g, 95% yield). ^{1}H NMR (400 MHz, Chloroform-d) δ 7.84 (d, J = 8.1 Hz, 2H), 7.40 (d, J = 8.2 Hz, 2H), 4.75 (d, J = 5.6 Hz, 2H), 4.48 (dd, J = 8.8, 1.9 Hz, 1H), 2.47 – 2.41 (m, 1H), 2.29 – 2.14 (m, 2H), 2.07 (s, 1H), 1.97 (s, 1H), 1.77 (d, J = 11.9 Hz, 1H), 1.34 (s, 3H), 1.28 (t, J = 7.1 Hz, 1H), 1.23 (d, J = 10.9 Hz, 1H), 0.92 (s, 3H). ^{13}C NMR (101 MHz, Chloroform-d) δ 143.94, 135.09, 126.14, 86.31, 78.27, 65.27, 60.44, 51.42, 39.54, 38.21, 35.57, 28.72, 27.12, 26.50, 24.07, 21.08, 14.22..

Synthesis of Pinacol Boronate (B)

Pinacol (3.35 g, 28.37 mmol) and 4-(hydroxymethyl)phenylboronic acid (4.31 g, 28.37 mmol) were stirred overnight with sodium sulfate (4.7 g) in THF (30 mL). Heterogenous solution was filtered via vacuum to separate sodium sulfate from finished product. The filtered solution was then concentrated in vacuo. The sample was then extracted with water (3 x 15 mL) and brine (3 x 10 mL) and dried over magnesium sulfate and filtered via gravity. The same extraction and subsequent filtration and concentration was performed again to further purify the sample. Product formed a thick, transparent oil. 1H NMR (400 MHz, DMSO-d6) δ 7.72 –

7.59 (m, 1H), 7.35 – 7.27 (m, 1H), 5.19 (t, J = 5.7 Hz, 0H), 4.53 (d, J = 5.7 Hz, 1H

Synthesis of cis-cyclopentane boronate

Cis-1,2-cyclopentanediol (1.05 g, 10.28 mmol) and 4-(hydroxymethyl)phenylboronic acid (1.56 g, 10.28 mmol) were stirred overnight with sodium sulfate (~1 g) in THF (15 mL). Mixture was filtered via gravity and concentrated in vacuo. Sample was purified using a Biotage ZIP 45 g silica column with 3:1 hexanes-ethyl acetate to achieve a white solid. Rf = 0.25 in 3:1 hexanes and ethyl acetate. 1H NMR (400 MHz, DMSO-d6) δ 7.65 (d, J = 8.0 Hz, 1H), 7.39 – 7.29 (m, 1H), 5.25 (t, J = 5.7 Hz, 0H), 5.03 – 4.97 (m, 1H), 4.53 (d, J = 5.7 Hz, 1H), 1.86 (ddt, J = 12.6, 7.2, 1.8 Hz, 1H), 1.71 – 1.42 (m, 2H).

Dihydroxylation of norborylene[41]

Norborylene (1.98 g, 20.88 mmol) was dissolved with stirring, on ice, in a solution of tert-Butyl alcohol and water (80 mL, 20 mL). Potassium permanganate (4.72 g, 29.88 mmol) was combined with sodium hydroxide (1.03 g, 25.68 mmol) in water (100 mL) and swirled by hand and then added dropwise through a separation funnel to the norborylene solution. This mixture was quenched with an aqueous sodium metabisulfite solution until colorless and then filtered through celite under vacuum. The sample was then extracted with ethyl acetate (4 x 120 mL) and the organics were combined and dried over magnesium sulfate and then filtered and

concentrated in vacuo. Finally, the resulting sample was recrystallized in hot toluene (10 mL) with stirring, forming colorless needles.

Synthesis of Norborene Boronate

Norbornenediol (0.245 g, 1.91 mmol) and 4-(hydroxymethyl)phenylboronic acid (0.290 g, 1.91 mmol) were combined with sodium sulfate (~0.5 g) in THF (8 mL) and stirred overnight. Solution was filtered, concentrated and purified in a column with 3:1 hexanes and ethyl acetate. The resulting product was concentrated in vacuo and on high vacuum to produce a white solid. Rf = 0.3 in 3:1 hexanes and ethyl acetate. 1H NMR (400 MHz, DMSO-d6) δ 7.70 – 7.62 (m, 1H), 7.35 (dq, J = 7.2, 0.9 Hz, 1H), 5.25 (t, J = 5.7 Hz, 0H), 4.53 (d, J = 5.7 Hz, 1H), 4.42 (d, J = 1.1 Hz, 1H), 2.29 (dt, J = 3.2, 1.6 Hz, 1H), 2.00 (s, 0H), 1.54 – 1.37 (m, 2H), 1.19 (dp, J = 10.8, 1.4 Hz, 1H), 1.10 (td, J = 7.7, 7.1, 2.2 Hz, 1H).

NMR-monitored transesterification of cyclopentane boronate and norbornene boronate with dextran

Cyclopentane boronate (9 mg) was dissolved in 783 μL deuterated dimethyl sulfoxide (d-DMSO). Norbornene boronate (10 mg) was dissolved in 783 μL d-DMSO. A standard ^{1}H-NMR was collected of each boronate sample. Then, each sample was combined with dextran in d-DMSO (50 mg/mL, 117 μL). ^{1}H-NMR spectra were collected at 0, 3, 21,

and 77 hours.

CHAPTER 3: THE SYNTHESIS OF PDB-DEX

3.1: Theory

PinB-Dex possessed major solubility issues as well as performance inefficiency upon microparticle formation. After synthesis, it lacked the ability to be easily re-dissolved in various organic solvents and the particles formed upon processing were inconsistent in size and shape (**Figure 18**). Ultimately, PinB-Dex was a difficult molecule to work with so the underlying reasons for its behavior were proposed and analyzed in the hopes of finding a solution or a better alternative. NMR analysis showed that the synthesis of PinB-Dex worked as planned so it was possible something about its structure was changing further downstream and could be causing the deficiencies in functionality. It was proposed that the principle issue with PinB-Dex is that adjacent molecules of the modified polymer were unexpectedly crosslinking with each other via a transesterification reaction (**Figure 19**).

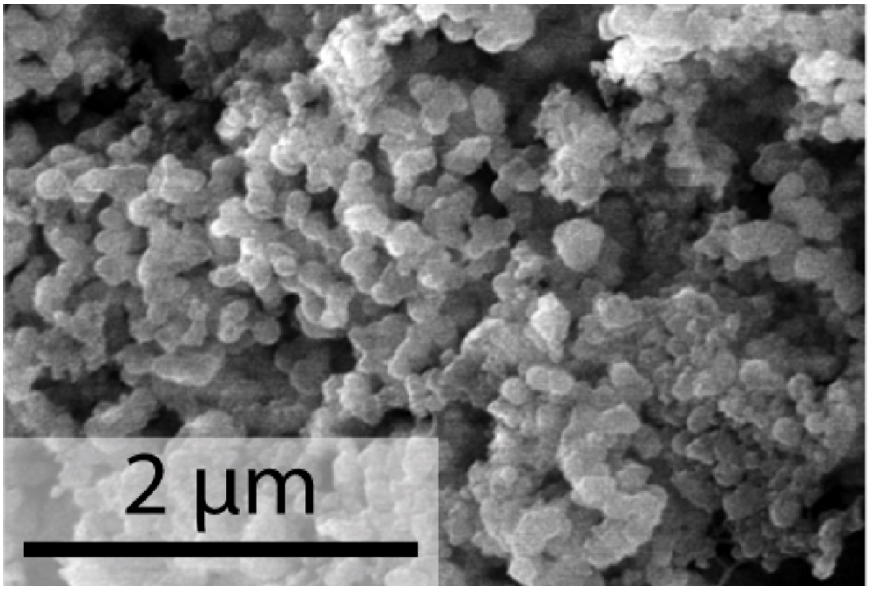

Figure 18. SEM Micrograph of PinB-Dex microparticles[31]

As addressed in the introduction, boronates exist in an equilibrium between their sp^2, trigonal planar form and their sp^3, tetrahedral form. This transition represents the structural shift that occurs when a boronic ester transesterifies, or switches from one type of ester to another. As described in the last chapter, NMR spectroscopy showed that a small amount of the pinacol modification was dissociating from the polymer, freeing up enough units of the boronic ester end to re-esterify with neighboring 4' – 6' hydroxyl pairs from anhydroglucose units. This action creates the cross-linking bridge between adjacent dextran polymers, which causes them to aggregate into a large mass, which would account for PinB-Dex's insolubility.

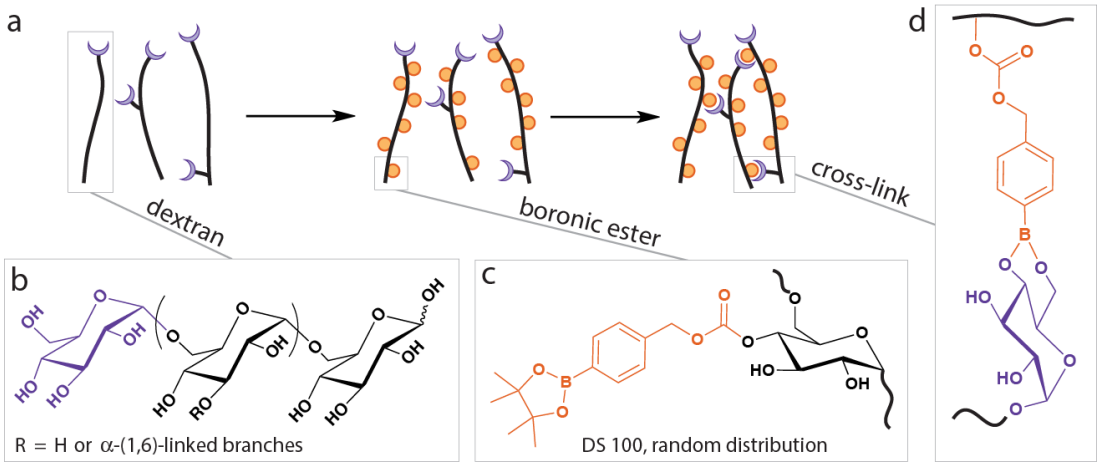

Figure 19. Transesterification of PinB-Dex with adjacent PinB-Dex units. a. After modification of dextran with boronic ester groups (orange circles), non-reducing ends (purple crescents) generate inter-strand links. b. Structure of dextran highlighting ~5% α-(1,3) branching. c. Structure of PinB modifications. d. Proposed linkage between polysaccharide non-reducing ends and boronic esters.

A closer look into the stability of boronic esters highlighted a correlation between the relative stability of pinacol boronic ester and pinanediol boronic ester. Boronic esters have been found to be most thermodynamically stable when formed with diols featuring rigid coplanar *cis*-1,2 diols.[39] Additionally, because transesterification occurs through an associative process, steric bulk has been observed to significantly slow the kinetics of transesterification. Among the most kinetically and thermodynamically stable boronic esters in the literature is that formed with pinanediol (PD), so it was substituted into PinB-Dex in place of pinacol.[39,42]

3.2: Results and Discussion

The synthesis of PDB-Dex occurs in three simple and high-yielding steps. The first step is the esterification of 4-(hydroxymethyl) phenylboronic acid with pinanediol, followed by activation to a carbamate by carbonyldiimidazole and finally, a second carbamate formation with dextran (**Scheme 4**). Each step of the synthesis required a set of purification protocols before the material proceeded to its next transformation. These were developed iteratively as the entire process was refined with the goal of producing the purest possible sample of PDB-Dex.

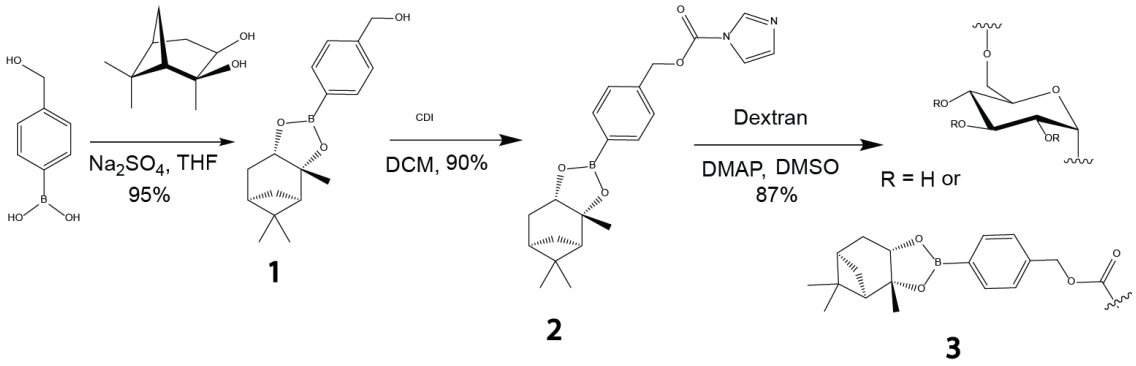

Scheme 4. Synthesis of PDB-Dex

It was found via thin layer chromatography (TLC) that after synthesis of pinane boronate **1,** excess, unreacted pinanediol frequently remained dissolved in the reaction flask causing impurities in the product. In order to cleanse the product of the excess reactant the entire product was purified through dry column chromatpgraphy (DCVC) using hexanes and ethyl acetate in a gradient elution.[43] DCVC was used in place of the

traditional route of flash chromatography, due to the large scale of the reaction. The TLC result post-column shows that the spot that initially appeared for pure pinanediol is no longer there, suggesting that the final product is likely one single molecule free of impurities (**Figure 20**).

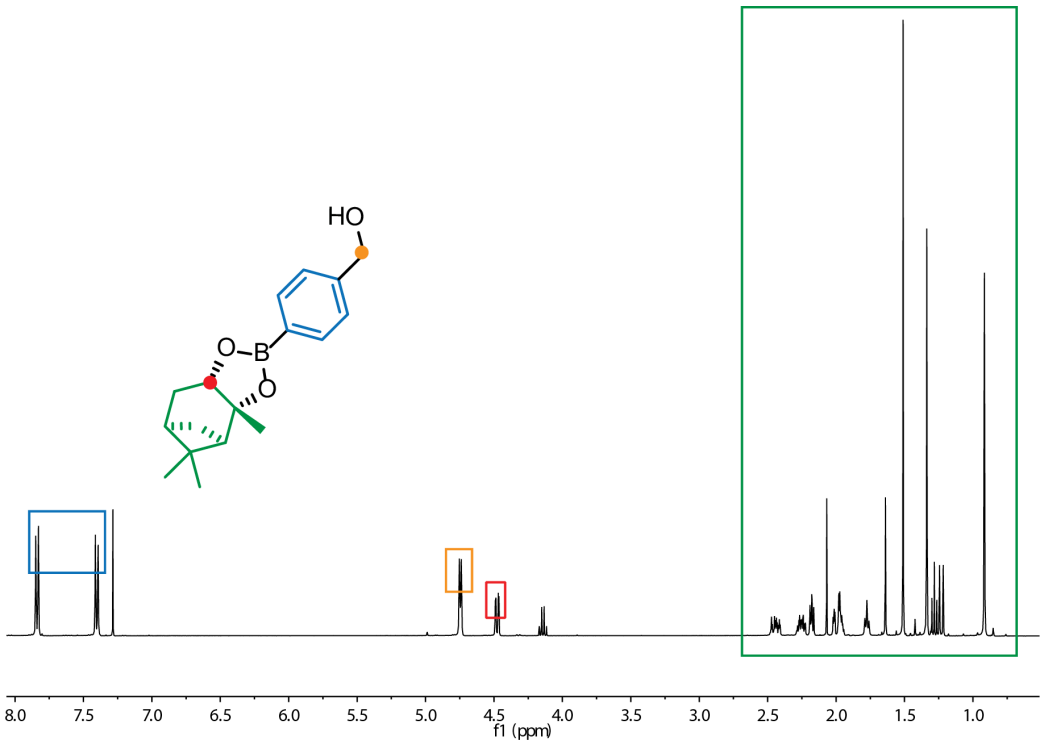

Figure 20. ^{1}H-NMR Spectrum of Pinane boronate with color coordinated labels

The second major purification step that occurs in the synthesis of PDB-Dex is an extraction after activation with carbonyldiimidazole to yield CDI-Activated Pinane Boronate **2** (**Figure 21**). The purpose of the activation reaction is to prepare the exposed alcohol group on the newly-formed boronate to form a carbamate that can eventually covalently bind with dextran. This reaction leaves imidazole behind as a byproduct, which can be extracted with a 5% $KHSO_4$ wash, followed by water, and then brine

(**Scheme 5).** Imidazole has a pKa of approximately 6.5-7 and can be protonated on the free nitrogen atom by $KHSO_4$ because the solution is inherently acidic. It is this interaction that pulls imidazole into the aqueous layer of the extraction, thus removing it from the organics.

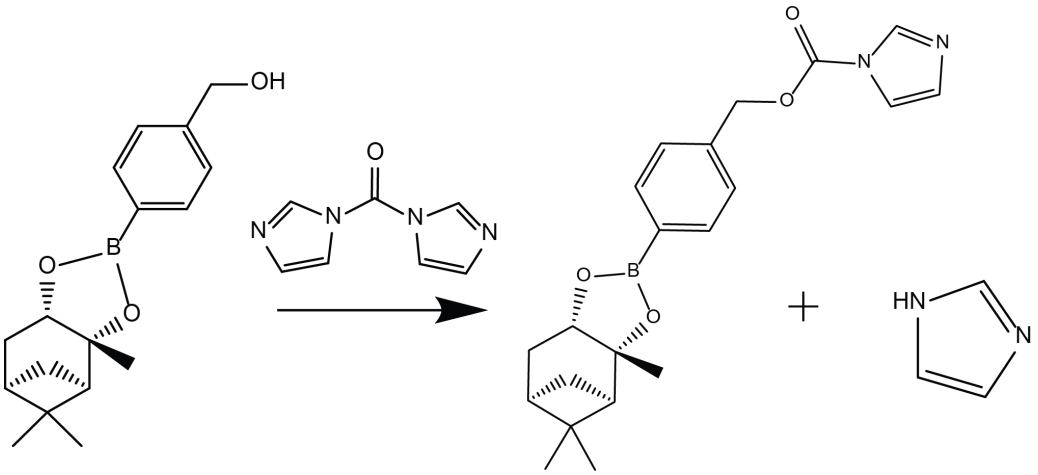

Scheme 5. Synthesis of CDI-Activated Pinane Boronate. Reaction yields an amide as well as imidazole as a byproduct.

The final step of the synthesis, which is the modification of dextran, requires a 3-step purification process that includes precipitation into 5% $KHSO_4$ to remove excess DMAP and more imidazole, the same extraction as performed previously on the activated carbamate product, and finally, re-precipitation into hexanes. The second precipitation into hexanes resulted from the discovery of latent pinanediol in the final product after extraction so a series of solubility tests was done to isolate an organic solvent that would dissolve pure pinanediol and precipitate the entire polymer to retrieve its solid form.

PDB-Dex was found to be soluble in various standard organic solvents such as ethyl acetate, toluene, chloroform, and acetone. This

alone gives it the ease of use and manipulation that previous iterations of its kind did not possess. Characterization of the final polymer via ^{1}H-NMR shows smooth "rolling hills" which is an indicator of a large polymer with little impurity (**Figure A5**).

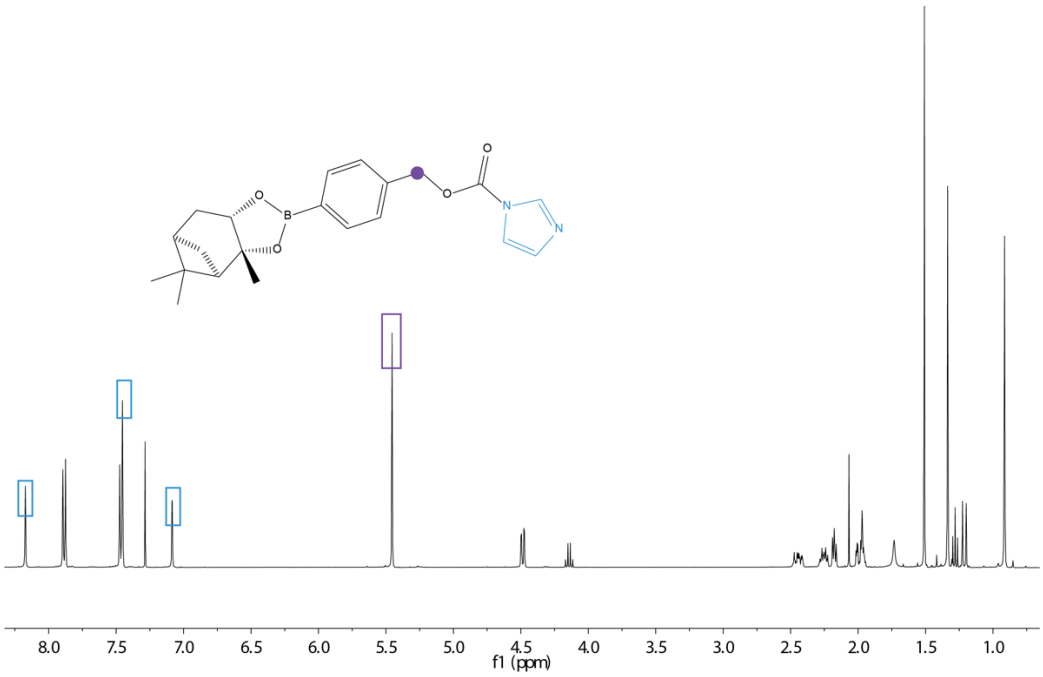

Figure 21. ^{1}H-NMR Spectrum of CDI-Activated Pinane boronate with color coordinated labels

3.3: Methods

Synthesis of Pinane Boronate **1**

(*1R, 2R, 3S, 5R*)-(-)-Pinanediol (4.83 g, 28.37 mmol) was combined with 4-(hydroxymethyl)phenyl boronic acid (4.31 g, 28.37 mmol) in tetrahydrofuran (43.2 mL). Sodium sulfate (7 g) was added to the reaction and stirred overnight. The solution was filtered and concentrated under vacuum. Dry column vacuum chromatography was used to purify the

product (0 – 80% EtOAc in Hex), Rf = 0.385. Fractions were combined and concentrated *in vacuo* to a pale yellow oil (7.6 g, 95% yield). ^{1}H NMR (400 MHz, Chloroform-d) δ 7.84 (d, J = 8.1 Hz, 2H), 7.40 (d, J = 8.2 Hz, 2H), 4.75 (d, J = 5.6 Hz, 2H), 4.48 (dd, J = 8.8, 1.9 Hz, 1H), 2.47 – 2.41 (m, 1H), 2.29 – 2.14 (m, 2H), 2.07 (s, 1H), 1.97 (s, 1H), 1.77 (d, J = 11.9 Hz, 1H), 1.34 (s, 3H), 1.28 (t, J = 7.1 Hz, 1H), 1.23 (d, J = 10.9 Hz, 1H), 0.92 (s, 3H). ^{13}C NMR (101 MHz, Chloroform-d) δ 143.94, 135.09, 126.14, 86.31, 78.27, 65.27, 60.44, 51.42, 39.54, 38.21, 35.57, 28.72, 27.12, 26.50, 24.07, 21.08, 14.22..

Synthesis of CDI Activated Pinane Boronate (CDI-PB) **2**

1 (7.6 g, 26.56 mmol) was dissolved in DCM (150 mL) in a dry flask under Ar, and then CDI (8.61 g, 53.11 mmol) was slowly added. After 30 minutes, the reaction was concentrated *in vacuo*, and redissolved in EtOAc (75 mL). This solution was washed with water (3 x 10 mL), 5% $KHSO_4$ (3 x 10 mL), and brine (2 x 10 mL). The organics were then dried over $MgSO_4$ and concentrated *in vacuo* to a thick, yellow oil (8.63 g, 86% yield). 1H NMR (400 MHz, Chloroform-d) δ 8.17 (t, J = 1.1 Hz, 1H), 7.89 (d, J = 8.1 Hz, 1H), 7.50 – 7.42 (m, 2H), 7.08 (dd, J = 1.7, 0.8 Hz, 1H), 5.45 (s, 1H), 4.49 (dd, J = 8.8, 1.8 Hz, 1H), 2.51 – 2.38 (m, 1H), 2.31 – 2.14 (m, 1H), 2.04 – 1.93 (m, 1H), 1.73 (s, 1H), 1.51 (s, 2H), 1.34 (s, 2H), 1.32 – 1.17 (m, 1H), 0.91 (s, 2H). 13C NMR (101 MHz, Chloroform-d) δ 148.59, 137.16, 136.71, 135.31, 130.71, 127.81, 117.16, 86.49, 78.38, 69.73, 60.40, 51.38, 39.51, 38.22, 35.53, 28.70, 27.10, 26.49, 24.06, 21.07, 14.22, 1.04.

Synthesis of PDB-Dex 3

In a dry flask under argon, dextran 9-10K (1.90 g, 11.70 mmol) was dissolved in DMSO (20 mL). **2** (8.90 g, 23.41 mmol) was added, and, after complete dissolution, DMAP (3.15 g, 25.75 mmol) was added. Solution was kept under Argon overnight. The solution was precipitated into 5% KHSO4 (~ 50 mL) and centrifuged (12,000 x g, 10 min) into a pellet. The supernatant was discarded and the resulting pellet was washed by resuspending in 5% $KHSO_4$ (40 mL), and centrifuging again. The pellet was then washed again with $KHSO_4$ (40 mL) and once with deuterated H_2O (d-dH_2O,30 mL). After discarding the supernatant, the pellet was frozen using liquid nitrogen and lyophilized. White solid was then redissolved in EtOAc (30 mL) and extracted with 5% $KHSO_4$ (3 x 10 mL), H_2O (2 x 10 mL), and brine (2 x 10 mL). The organic phase was dried over $MgSO_4$, filtered, and then precipitated dropwise into hexanes (100 mL), pelleted via centrifugation and concentrated *in vacuo* to yield a white solid (4.8 g, 83% yield).

Characterization of degradation byproducts by NMR

To prep the sample, PDB-Dex was dissolved in deuterated PBS (0.2mg/mL, pD 7.4, 10mM) and combined with 50 mM Na_2O_2. A standard proton NMR was run for 60 hrs and 64 scans were taken every 10 minutes.

CHAPTER 4: THE MECHANICS OF PDB-DEX

4.1: Theory

Once the synthesis of PDB-Dex polymer was refined and the material was deemed cooperative in its behavior, its degradation pathway and ability to be processed into particles was tested. As previously described in the introduction, oxidation is a very useful trigger condition because it is ubiquitous in dendritic cells and many other places in the body. It has also been suggested that it could be a better trigger than acidity because the pH of lysosomes in dendrites is actually neutral or even slightly higher.[19]

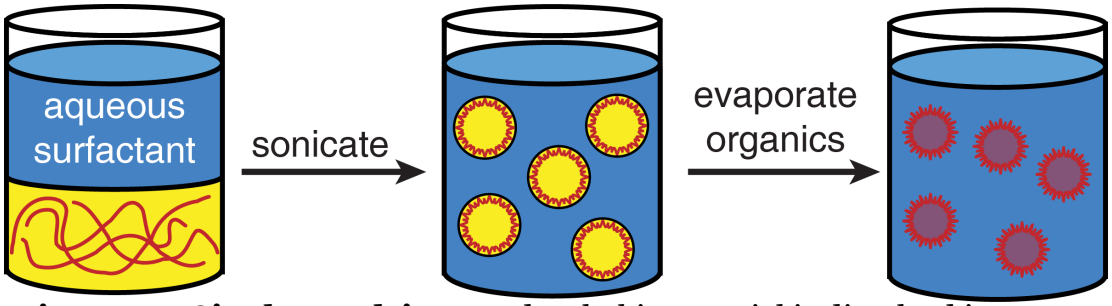

Figure 22. Single emulsion. Hydrophobic material is dissolved in an organic solvent and sonicated in the presence of an aqueous surfactamt, forcing the formation of spherical particles of the primary material. The organics are then left to evaporate from the suspension.

There are a number of ways microparticles can be produced. One commonly used for biodegradable polymeric materials is double emulsion.

There are many variations and derivatives of double emulsion that suit particular materials and goals based on behavior and conditions. Briefly, this technique involves utilizing the material's inherent properties in organics and aqueous solvents to encourage droplet formation. The appropriate protocol for a multistep emulsion process greatly depends on the hydrophobicity and hydrophilicity of the material in question.[44] An emulsion typically contains two phases: dispersed phase and continuous phase. It follows that the dispersed phase is dispersed into the continuous phase. There are two main types of double emulsion involving water (w) and oil (o) : w/o/w or o/w/o. In the former case, water is dispersed in oil which is then dispersed in water and in the latter they are reversed. Customarily, o/w/o is used for hydrophobic materials. However, it does not suit hydrophilic materials because they may diffuse into the continuous phase or be insoluble in organic solvents.[45] The goal of double emulsion is to process a material, typically polymeric, into particles and subsequently encapsulate another material such as a drug or protein. For the purposes of solely creating empty microparticles, the first half of double emulsion, can be referred to as single emulsion and carried out separately (**Figure 22**).

To make microparticles using a single emulsion, a solution of the desired material is prepared and then combined with an aqueous surfactant and then sonicated to create the emulsion. After sonication, the organics can be evaporated and the newly formed microparticles can be isolated via centrifugation and eventually lyophilization.

4.2: Results and Discussion

The efficiency and mechanism of degradation of PDB-Dex was assessed via NMR. NMR requires highly concentrated solutions of material, which can be difficult to obtain, but it is useful because it could show changes in PDB-Dex's composition over time as it was exposed to peroxide. We suspended PDB-Dex particles in deuterated PBS and added Na_2O_2, conditions which mimicked a biological environment and scanned the material for 2.5 days. From this we were able to obtain a clear picture of the self-immolative degradation mechanism that the polymer followed and determine the rate-limiting step (**Figure 23a**).

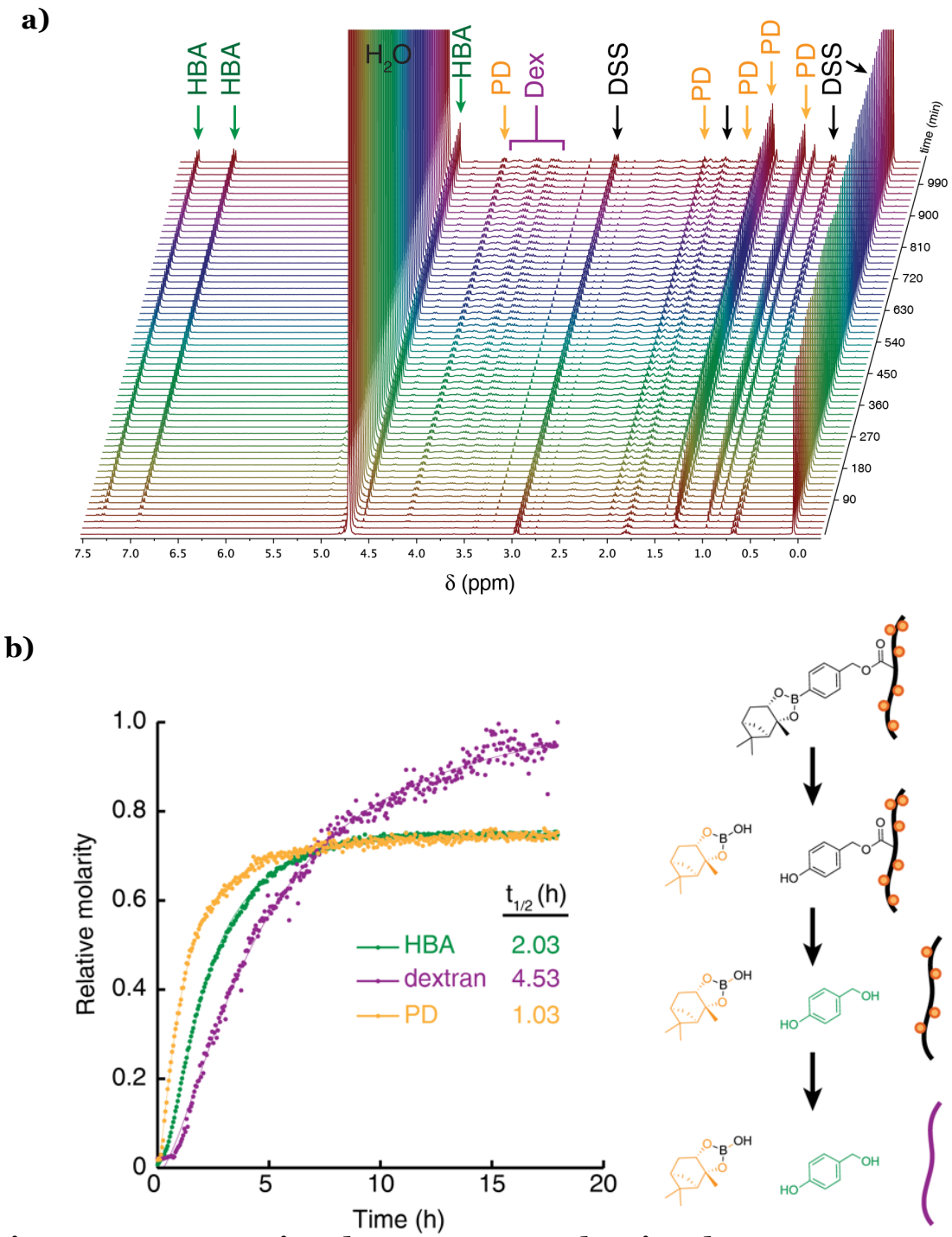

Figure 23. ^{1}H-NMR time-lapse spectrum showing the degradation mechanism of PDB-Dex. a. NMR spectrum used to obtain the graph below. Appearance of peaks for byproducts can be seen over time b. Graph of integrations of main degradation components derived from the above spectrum

The first part of the molecule to cleave is the pinanediol-boron complex (PD) and it does so through hydrolysis from the rest of the polymer. It hasn't been confirmed whether PD and boron dissociate separately or together as a complex as shown, but the NMR shows that both components cleave at the same time, so the complex is likely. The second moiety to cleave is 4-hydroxybenzyl alcohol (HBA) and once that has occurred, pure dextran remains (**Figure 23b**). The new PD and the resulting HBA increase their concentrations at relatively the same rate and their concentrations stay at a ratio of 1:0.7 PD to HBA. They are physically linked to each other so the fact that their concentrations coincide is expected. As for the speed of cleavage, the half-life of HBA is approximately double that of PD suggesting that it remains bound to the dextran backbone longer. Here, the rate-limiting factor is the cleavage of PD, which occurs within the first few hours of exposure to H_2O_2. Once that has occurred, it opens the rest of the modification on dextran to cleave as well (**Scheme 1**)**.** This entire mechanism occurs within the first 20 hours of exposure to oxidative conditions and after that point, the concentrations of the byproducts hit their capacity. NMR as a technique in this context requires concentrations of peroxide and polymer that are both high and stoichiometrically proportional to each other, but not biologically relevant.

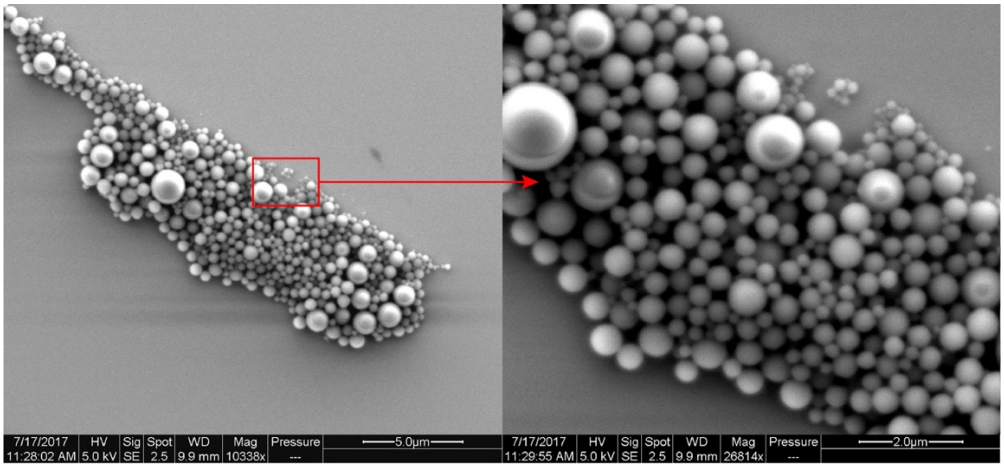

Figure 24. SEM Micrograph of PDB-Dex Microparticles. Suspension of particles were drop-cast onto silicon wafers and sputter coated with ~5 nm of a palladium/gold alloy then imaged at 5.0 kV in Secondary Electrons mode.

After analyzing the mechanism of degradation of PDB-Dex particles, they were imaged and measured for size. Compared to PinB-Dex, the particles formed were consistently spherical and on a large scale, consistent in size (**Figure 24**). Our choice of emulsion as a mode of processing is likely what generated spherical particles, which is a common and useful shape for biocompatible materials. PDB-Dex microparticles are easily suspended which indicates the particles are discreet, unlike previously with their PinB-Dex composition as shown in SEM images (**Figure 18**).

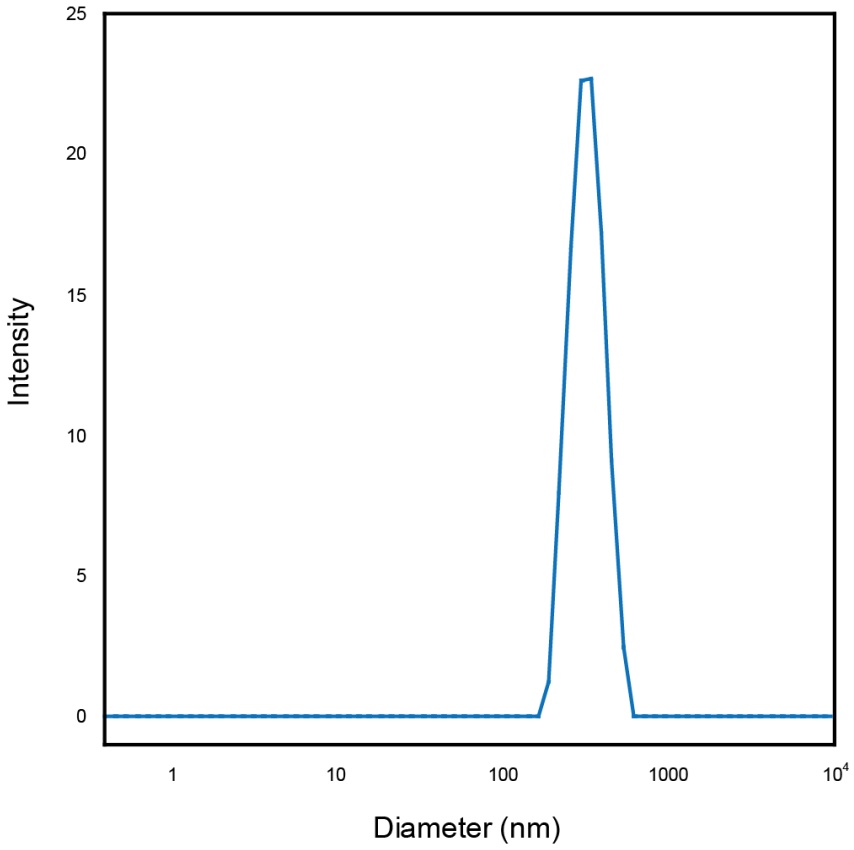

Figure 25. DLS Measurement of average particle size. PDB-Dex was suspended in PBS (0.1 mg/mL), lightly sonicated and transferred to a standard disposable polystyrene cuvette. Measurements were taken at 37˚C.

Dynamic light scattering (DLS) measured an average particle size of 331 ± 173 nm (**Figure 25**). Particle size varied however between different batches of PDB-Dex microparticles. DLS measurements presented several issues in producing consistent results. This could be because DLS measures Brownian motion and if true Brownian motion were occurring, the particles would never settle.[46] However, because the sample is an aqueous suspension, it does settle over time and the result is highly varied measurements, making it difficult to extract an average. Dust and debris collection in the samples also skews the measurements as the machine has

difficulty discerning the difference between those particles and particles of interest.

In order to measure degradation at an environment that better mimics an organism, the concentration of H_2O_2 had to be lowered as close as possible to the scale that it would be inside lysosomes as possible. While NMR rendered a clear picture of the degradation mechanism of PDB-Dex, the concentration of peroxide used to achieve this result was far too high to be considered "natural". This concentration was necessary, however, to yield NMR signals that were strong enough to be analyzed. Thus, other methods for monitoring degradation of PDB-Dex particles were explored. The first assay that was tested was a colorimetric assay that employed anthrone and sulfuric acid as the reagents for detecting carbohydrate appearance.[47] In theory, this method was supposed to show how much carbohydrate (pure dextran) accumulated throughout the degradation process of samples of microparticles. This was achieved by preparing solutions of undegraded polymer in PBS and exposing them to various concentrations of H_2O_2. Those samples were then lightly mixed for approximately two days while small aliquots were collected every few hours and subsequently each quenched. That yielded samples of PDB-Dex at different points in the course of the degradation reaction that could then be mixed with an anthrone-sulfuric acid solution, which was specifically designed to tag carbohydrates as they appear in solution. Unfortunately, the assay was not sensitive enough to detect the reaction, demonstrated by the lack of color change throughout the plate.

A 3-component bicinchoninic assay was tested to replace the anthrone-sulfuric acid assay, which ultimately rendered promising results (**Figure 26a**). In a normal BCA Assay, peroxide would interfere with the detection of protein, but that obstacle was overcome through catalytic decomposition of H_2O_2 with potassium iodide. The data extracted from this assay shows that the degradation behavior of PDB-Dex when exposed to H_2O_2 is dose-dependent (**Figure 26b**). Specifically, as the concentration of peroxide increases, the degradation occurs faster. It also showed that degradation can occur with concentrations as low as 0.01 mM H_2O_2.

a)

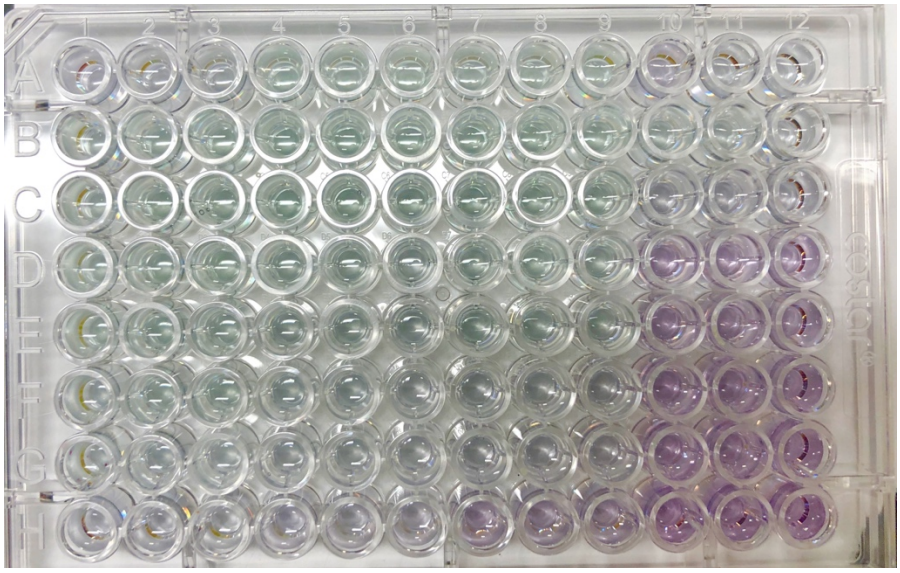

b)

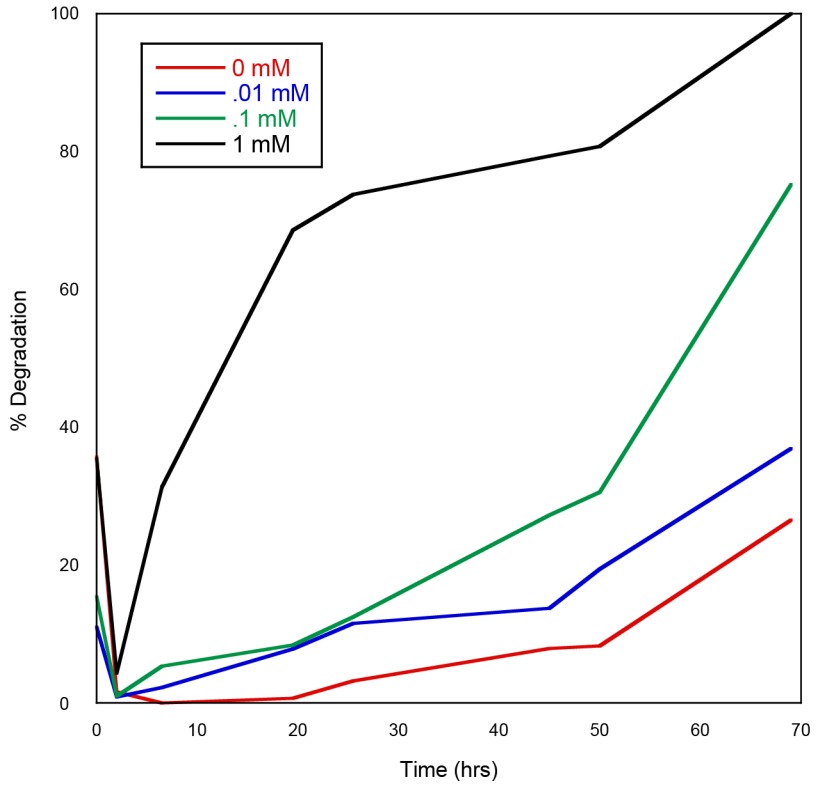

Figure 26. BCA Assay Plate and results. a) 96 well polystyrene plate with 4 H_2O_2 conditions increasing from left to right. Each condition was plated in triplicate. Vertical axis of plate from top to bottom represents timepoints in increasing order. b) Percent degradation obtained from values of intensity of color measured by a Spectramax M5 plate reader.

4.3: Methods

Preparation of Microparticles

Sub-micron Single Emulsion Particles were prepared according to a procedure adapted from Beaudette et al.[48] Briefly, PDB-Dex (100 mg) was dissolved in dichloromethane (2 mL). This solution was added to an aqueous solution of poly(vinyl alcohol) (PVA, MW = 13,000 -23,000 g/mol, 87-89% hydrolyzed) (6 mL, 1% w/w in PBS) and emulsified by sonicating for 45 s on ice using a probe ultrasonicator (with the following settings: 45 s total sonication cycling between 0.8 s on and 0.2 s off with power at 35% and using a 1/2- inch flat tip. The resulting emulsion was poured into a second PVA solution (100 ml, 0.3% w/w in PBS) and stirred for 5.5 h allowing the organic solvent to evaporate. The particles were isolated by centrifugation (14,000 x g, 5 min) and washed with dd-H_2O by vortexing and sonication followed by centrifugation and removal of the supernatant. The washed particles were resuspended in dd-H_2O and lyophilized to yield a white solid (60 mg, 60% yield).

Dynamic light scattering

PDB-Dex was suspended in PBS (0.1 mg/mL), lightly sonicated and transferred to a standard disposable polystyrene cuvette. Measurements were taken at 37˚C.

Scanning electron microscopy

Microparticles were characterized by scanning electron microscopy using a Quanta 200 SEM (FEI, USA). Particles were suspended in dd-H_2O at a concentration of 1 mg/mL and the resulting dispersions were dripped onto silicon wafers. After 15 min, the remaining water was wicked away using the corner of a KimWipe and the samples were allowed to air dry. The particles were then sputter coated with ~5 nm of a palladium/gold alloy and imaged at 5.0 kV in Secondary Electrons mode.

NMR measurement of degradation kinetics

To prep the sample, PDB-Dex particles were dissolved in deuterated PBS (0.1 mg/mL, 1x, pH 7.4) and combined with 1 mM Na_2O_2. H^1 - NMR was run for 60 hrs, measured every 10 min.

Bulk Degradation of Microparticles

PDB-Dex particles were suspended at a concentration of 5 mg/mL in 1 mL solutions of PBS containing 0 mM, 0.01 mM, 0.1 mM, or 1 mM H_2O_2 in triplicate. These samples were placed on an Eppendorf Thermomixer-R (Fisher Scientific, USA) heating block with shaking at 37˚C Aliquots were taken over the course of the following 70 hours, centrifuged at 10,000 x g for 30 s and the supernatant was stored at 4˚C.

BCA Assay

A Thermo Scientific Micro Bicinchoninic Assay was performed according to the manufacturer protocol with slight alterations. Briefly, 50 mL of working reagent (WR) was prepared from a 25:24:1 volume ratio of Reagents A, B, and C (1 mL). In a 96-well polystyrene microplate, supernatants of aliquots taken from degrading microparticle suspensions (above, 50 uL) were mixed with 1% KI (20 uL) to catalytically quench residual H_2O_2. After 3 h, WR was added (200 uL). The plate was then incubated at 37°C for 3 hours and absorbance was measured at 562 nm on a Spectramax M5 plate reader by Molecular Devices.

CHAPTER 5: BIOLOGICAL APPLICATIONS OF PDB-DEX

5.1: Theory

Biological efficacy is a vital property of any drug delivery material. The primary behaviors of interest for PDB-Dex as a potential vehicle for immunostimulatory agents is its encapsulation efficiency, cytotoxicity, and ability to deliver a drug to a specified target. These properties can be tested in many different ways and with a variety of drugs and proteins. Biological viability experiments were carried out by the Ainslie Lab at the University of North Carolina Eshelman School of Pharmacy in Chapel Hill, NC.

The Ainslie Lab processed PDB-Dex into microparticles through electrospraying, which is a commonly used technique that harnesses electrical charge to evenly distribute substances onto surfaces on a microscopic scale. To create polymer-based particles, the material is dissolved in organics and syringe-pumped onto an electrically charged plate. Once the particles have formed, the organics are evaporated off of the surface. To create drug-loaded particles, a solution of the polymer and the desired drug is prepared and sprayed in the same manner as the "empty" polymer.

To assess cytotoxicity, a 3-(4,5-dimethylthiazol-2-yl)-2,5-diphenyltetrazolium bromide (MTT) assay was employed. An MTT assay is

a colorimetric assay that measures metabolic activity by utilizing the reducing power of NAD(P)H-dependent cellular oxidoreductase enzymes that are present in cells, and therefore indicate the amount of viable cells present under certain conditions.[49] These enzymes are capable of reducing MTT dye to an insoluble form that has a purple hue. Therefore, the darker the purple hue that appears in plate wells, the more viable cells are present.

In vitro studies consisted of an enzyme-linked immunosorbent assay (ELISA) that measured the secretion of immune response-triggering molecules in viable cells. ELISA is a colorimetric assay that uses relationships between specific antigens and antibodies to quantify the presence of a particular molecule in a sample. In short, antigens from the sample are attached to a surface and that surface is then coated with the corresponding antibodies that have been linked to an enzyme. The surface is then exposed to a substance that contains a substrate for that enzyme and the binding between the enzyme and its substrate produces a detectable signal in the form of a color change.[50]

5.2: Results and Discussion

Microparticles used in these studies were prepared via electrospray (ES MPs) and were loaded with Resiquimod (Resi), a hydrophobic adjuvant that targets toll-like receptor 7 and 8. Encapsulation efficiency was measured to be 59% (**Figure 27**).

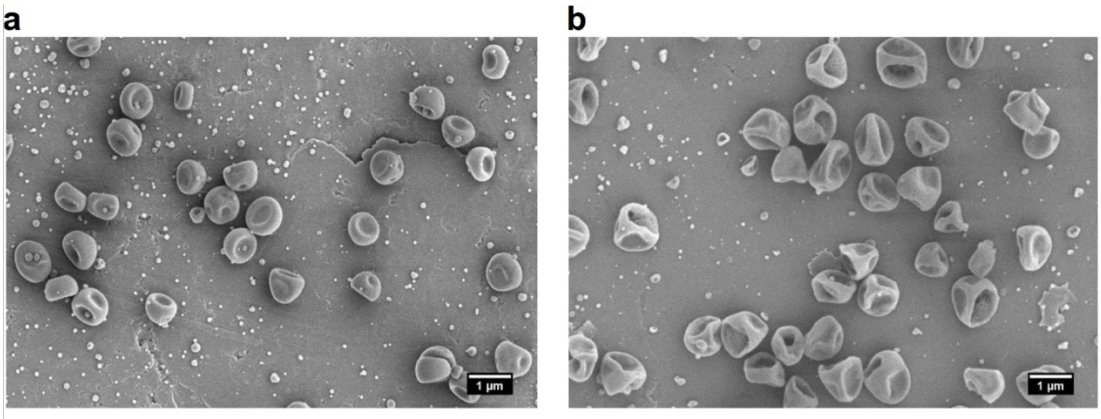

Figure 27. SEM images of PDB-Dex Microparticles of (**a**) blank and (**b**) resiquimod-loaded PDB-Dex ES MPs.

Cytotoxicity was assessed by examining cell viability of murine bone marrow-derived dendritic cells (BMDCs) when exposed to unloaded and resiquimod-loaded PDB-Dex ES MPs (**Figure 27**). Cell viability of BMDCs remained at high levels that mirrored the control levels, showing that PDB-Dex has virtually no negative effect on the vitality of cells. Additionally, it can be observed that Resi-loaded PDB-Dex ES MPs were less toxic at lower concentrations of Resi (**Figure 28**).

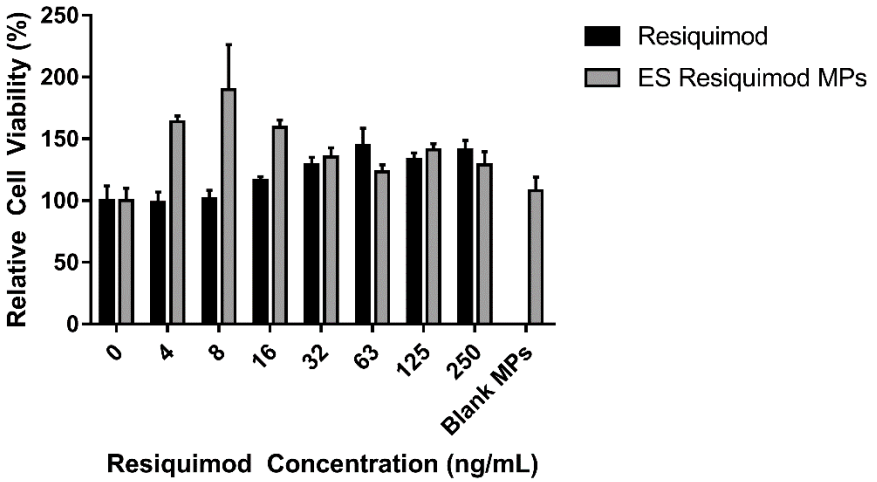

Figure 28. Cytotoxicity screening of electrosprayed PDB-Dex particles. BMDCs were treated with blank PDB-Dex MPs as a control or a range of concentrations of free resiquimod or resiquimod-loaded PDB-Dex ES MPs (5.9 μg resi/mg MP) for 72 hours, and an MTT assay was used to determine cell viability. Viability remained high across all treatment groups.

In vitro cell signaling was observed through the use of ELISA that measured the secretion of proinflammatory cytokines IL-6 and TNF-α when BMDCs were exposed to resiquimod-loaded PDB-Dex particles (**Figure 29**). Cells exposed to loaded particles exhibited similar but slower rates of secretion of both cytokines which was proposed to have occurred due to the controlled release of payload that begins initially through diffusion of particles into the BMDCs and eventually switches to oxidation-mediated degradation. This theory is supported by the increase in IL-6 secretion in particle-treated cells after 24 hours compared to the decrease apparent in free drug-treated cells.

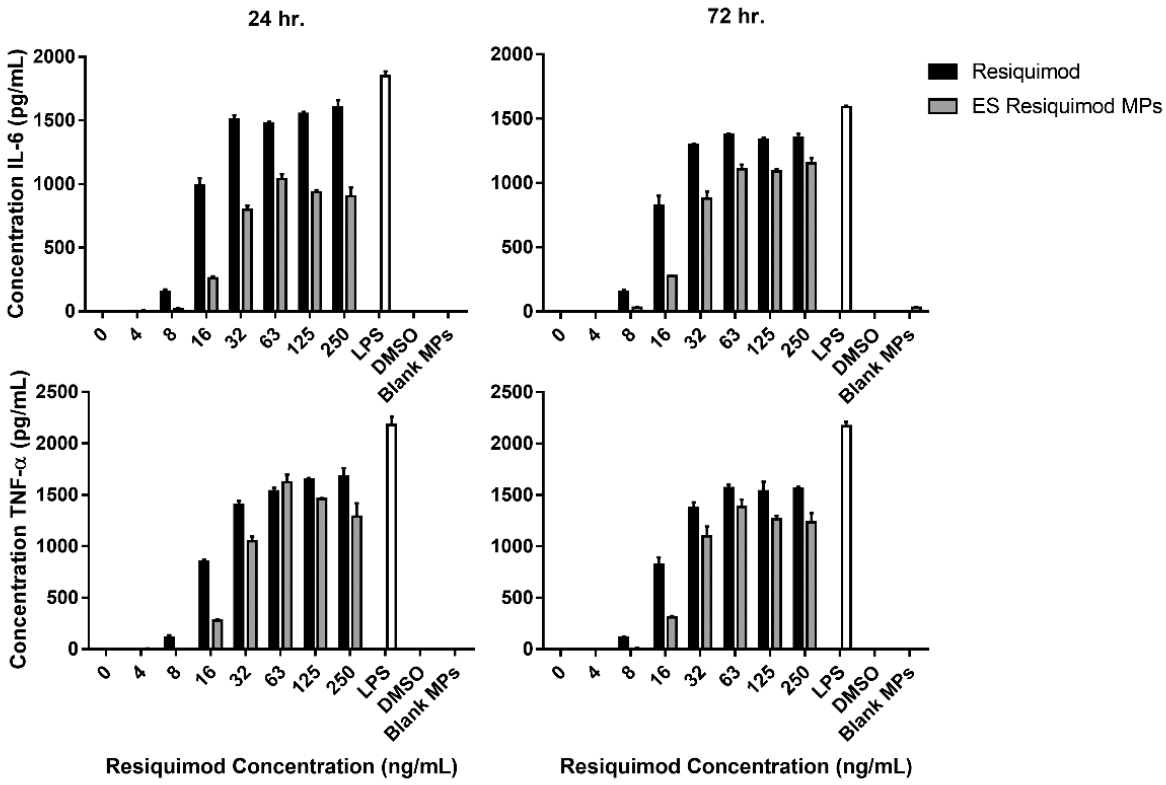

Figure 29. Measurement of PDB-Dex's ability to trigger excretion of proinflammatory cytokines. BMDCs were treated with blank PDB-Dex MPs or a range of concentrations of free resiquimod or resiquimod-loaded PDB-Dex MPs for 24 and 72 hours, and their secretion of proinflammatory cytokines IL-6 and TNF-α was quantified by ELISA.

5.3: Methods

Electrosprayed PDB-Dex MPs

PDB-Dex was purified by dissolution in THF and centrifugation at 22,000 x g for one hour**.** The supernatant was removed and transferred into a scintillation vial where it was then placed in a rotary evaporator and subsequently lyophilized to remove all residual water and THF. Resiquimod-loaded PDB-Dex MPs were fabricated using an electrohydrodynamic spraying (ES) method similar to that previously

reported.[51] A stainless steel plate was exposed to UV light for 1 hr and heat treated at 265° C for 1 hour to sterilize and reduce any endotoxin. PDB-Dex and resiquimod (1% total wt. solids) were dissolved in a 95:5 ethyl acetate:butanol mixture. A syringe pump was used to pump the resulting solution through an 18 gauge needle mounted over the steel plate with a flow rate of 0.2 mL/hour. The needle and steel plate were charged at -5 kV and +2.5 kV, respectively, using high voltage power sources (Gamma High Voltage Research Inc., Ormond Beach, FL). MPs were collected on the plate for 12.5 hours. PDB-Dex blank MPs were fabricated by the same process without resiquimod in the sprayed solution.

Resiquimod quantification

Resiquimod-loaded PDB-Dex MP loading was quantified by measuring fluorescence.[51] Samples were prepared in triplicate and dissolved in DMSO. These were loaded onto a solvent resistant 96-well plate and quantified using a standard curve generated from free resiquimod in DMSO based on fluorescence (excitation: 260 nm, emission 360 nm) using a SpectraMax M2 microplate reader. Blank PDB-Dex MPs were used to measure the background signal which was subtracted from MP-containing wells. Encapsulation efficiency of Resiquimod in PDB-DEX MPs was calculated as shown:

$$Encapsulation\ efficiency(\%) = \frac{Experimental\ resiquimod\ loading}{Theoretical\ resiquimod\ loading} \times 100$$

In vitro cell viability analysis

Balb/c mouse (Jackson Laboratory, Bar Harbor ME) bone marrow derived dendritic cells (BMDCs) were prepared and cultured using a previously published protocol.[52] Metabolic activity (viability and proliferation) of BMDCs was analyzed using a 3-(4,5-dimethylthiazol-2-yl)-2,5-diphenyltetrazolium bromide (MTT) assay after treatment with resiquimod or resiquimod-loaded PDB-Dex MPs at concentrations ranging from 0 to 250 ng resiquimod/mL. Cells were seeded in 200 μL of media overnight in a 96-well plate at 25,000 cells per well before incubation. They were then treated with different experimental groups for 72 hours. Cells treated with blank PDB-Dex MPs, DMSO at maximum concentration, media only, or lipopolysaccharide (LPS, 100 ng/mL) were included as controls. The supernatant was removed and retained for future use. MTT solution (0.5 mg/mL) was added to each well (150 μL), including 3 blank wells (media only). The plate was incubated at 37°C for 1 hour. Media was removed from each well, and formazan crystals were dissolved in 100 μL of isopropanol. The absorbance of the resultant solution was measured at 560 nm using a SpectraMax M2 microplate reader. The background absorbance at 670 nm was also measured and subtracted from every well. Blank wells (media only) also served as background.

Cytokine quantification

BMDCs were prepared and cultured with the same method cited above. Secretion of IL-6 and TNF-α from BMDCs was analyzed by ELISA after treatment with resiquimod or resiquimod-loaded PDB-Dex MPs at doses ranging from 0 to 250 ng/mL. Cells were seeded in 200 μL of media overnight in a 96-well plate at 25,000 cells per well before incubation with different treatment groups for 24 or 72 hours. Cells treated with equivalent masses of blank PDB-Dex MPs, media only, or lipopolysaccharide (LPS, 100 ng/mL) were included as controls. The supernatants from the 24 and 72 hour conditions were collected and analyzed for IL-6 and TNF-α according to the manufacturer's instructions (Fisher Scientific, Hampton, NH).

Conclusions

The use of arylboronates as capping moieties on dextran in a solubility-altering mechanism is an underdeveloped concept in the field of drug delivery materials. This work presents a new material for immunotherapy applications that is biocompatible, biodegradable, and capable of encapsulating and delivering drug and protein payloads for interaction with the immune system. It is an easily and safely synthesizable material that degrades via a self-immolative sequence. PDB-Dex microparticles produced through emulsion are smooth, spherical, and consistent in size around 250 nm, which is similar to previous reports using the same technique.

The full degradation of particles can take 20 hours or more, which does not necessarily mimic the time frame of all potential immune-triggering application of the material. However, a slow-release mechanism could be fitting for specific cases, with the wide range of drug-target pathways and therapeutic methods that PDB-Dex could be compatible with.

The direct comparison between pinanediol, pinacol, cyclopentanediol, and norbornediol presents new insight on the effect of diol variation on ester formation with phenylboronic acid derivatives. Replacing the pinacol in PinB-Dex with pinanediol to create PDB-Dex remedied the interchain crosslinking that occurred as a result of pinacol's inability to form a hydrolytically stable boronic ester. It has been established in literature that rigid, cyclic diols form the most stable

boronic esters. This study has confirmed that pattern and applied it to the context of behavior-altering modifications to dextran. Through an NMR-monitored transesterification experiment it was established that the usage of pinacol boronate lead to the most tranesterifcation, followed by cyclopentane boronate, then norbornene boronate, and finally, PD boronate rendered no evidence of unwanted transesterification. Pinacol is not rigid, cyclic or sterically hindered relative to PD, which would explain its contribution to transesterification. Cyclopentane is cyclic and rigid, but is the least sterically hindered out of the 3 cyclic, rigid diols tested, which explains its place in the ranking. Norbornene is slightly more sterically hindered than cyclopentane and pinanediol is the most sterically hindered out of all four, which supports its behavior as a stable boronate that has eradicated the transesterification and crosslinking obstacle that previously inhibited this class of polymer's functionality.

The pattern that has been established can be applied to a range of other diols that are candidates for stable ester formation. Efforts to expand the study beyond the diols featured in this thesis are under way. Specifically, various nopol derivatives are being evaluated for efficacy in this context. It is possible that there is a diol that works more efficiently than pinanediol and could improve the system of an arylboronate-modifed dextran polymer even more. We have shown that the behavior of each diol varies based on structural characteristics, so it is also possible that unexplored diols could tune dextran to simply have *different* and equally useful properties from PDB-Dex.

References

(1) van Vlerken, L. E.; Vyas, T. K.; Amiji, M. M. Poly(Ethylene Glycol)-Modified Nanocarriers for Tumor-Targeted and Intracellular Delivery. *Pharm. Res.* **2007**, *24* (8), 1405–1414. https://doi.org/10.1007/s11095-007-9284-6.

(2) Galvin, P.; Thompson, D.; Ryan, K. B.; McCarthy, A.; Moore, A. C.; Burke, C. S.; Dyson, M.; MacCraith, B. D.; Gun'ko, Y. K.; Byrne, M. T.; et al. Nanoparticle-Based Drug Delivery: Case Studies for Cancer and Cardiovascular Applications. *Cell. Mol. Life Sci.* **2012**, *69* (3), 389–404. https://doi.org/10.1007/s00018-011-0856-6.

(3) Broaders, K. E.; Cohen, J. A.; Beaudette, T. T.; Bachelder, E. M.; Frechet, J. M. J. Acetalated Dextran Is a Chemically and Biologically Tunable Material for Particulate Immunotherapy. *Proc. Natl. Acad. Sci.* **2009**, *106* (14), 5497–5502. https://doi.org/10.1073/pnas.0901592106.

(4) Le, J. Drug Absorption. *Merck Manual (Professional Version)*; 2017.

(5) Santini Jr, J. T.; Cima, M. J.; Langer, R. A Controlled-Release Microchip. *Nature* **1999**, *397*, 335.

(6) Farra, R.; Sheppard, N. F.; McCabe, L.; Neer, R. M.; Anderson, J. M.; Santini, J. T.; Cima, M. J.; Langer, R. First-in-Human Testing of a Wirelessly Controlled Drug Delivery Microchip. *Sci. Transl. Med.* **2012**, *4* (122), 122ra21. https://doi.org/10.1126/scitranslmed.3003276.

(7) Chertok, B.; Langer, R. Circulating Magnetic Microbubbles for Localized Real-Time Control of Drug Delivery by Ultrasonography-Guided Magnetic Targeting and Ultrasound. *Theranostics* **2018**, *8* (2), 341–357. https://doi.org/10.7150/thno.20781.

(8) Cheng, R.; Meng, F.; Deng, C.; Klok, H.-A.; Zhong, Z. Dual and Multi-Stimuli Responsive Polymeric Nanoparticles for Programmed Site-Specific Drug Delivery. *Biomaterials* **2013**, *34* (14), 3647–3657. https://doi.org/10.1016/j.biomaterials.2013.01.084.

(9) Senapati, S.; Mahanta, A. K.; Kumar, S.; Maiti, P. Controlled Drug Delivery Vehicles for Cancer Treatment and Their Performance. *Signal Transduct. Target. Ther.* **2018**, *3* (1), 7. https://doi.org/10.1038/s41392-017-0004-3.

(10) Blau, H. M.; Springer, M. L. Gene Therapy — A Novel Form of Drug Delivery. *N. Engl. J. Med.* **1995**, *333* (18), 1204–1207. https://doi.org/10.1056/NEJM199511023331808.

(11) Duncan, R. Drug-Polymer Conjugates: Potential for Improved Chemotherapy. *Anticancer. Drugs* **1992**, *3* (3), 175–210.

(12) Watson Levings, R. S.; Smith, A. D.; Broome, T. A.; Rice, B. L.; Gibbs, E. P.; Myara, D. A.; Hyddmark, E. V.; Nasri, E.; Zarezadeh, A.; Levings, P. P.; et al. Self-Complementary Adeno-Associated Virus–Mediated Interleukin-1 Receptor Antagonist Gene Delivery for the Treatment of Osteoarthritis: Test of Efficacy in an Equine Model. *Hum. Gene Ther. Clin. Dev.* **2018**, *29* (2), 101–112. https://doi.org/10.1089/humc.2017.143.

(13) Murphy, K. P. *Janeway's Immunobiology*, 8th ed.; Garland Science, Taylor & Francis Group, LLC: New York, New York, 2012.
(14) Okada, C. Y.; Rechsteiner, M. Introduction of Macromolecules into Cultured Mammalian Cells by Osmotic Lysis of Pinocytic Vesicles. *Cell* **1982**, *29* (1), 33–41. https://doi.org/10.1016/0092-8674(82)90087-3.
(15) Miller, K. R.; Levine, J. *Prentice Hall Biology*; Pearson Prentice Hall, 2005.
(16) Sies, H. Oxidative Stress: A Concept in Redox Biology and Medicine. *Redox Biol.* **2015**, *4*, 180–183. https://doi.org/10.1016/j.redox.2015.01.002.
(17) Schieber, M.; Chandel, N. S. ROS Function in Redox Signaling and Oxidative Stress. *Curr. Biol.* **2014**, *24* (10), R453–R462. https://doi.org/10.1016/j.cub.2014.03.034.
(18) Brigelius-Flohé, R.; Flohé, L. Basic Principles and Emerging Concepts in the Redox Control of Transcription Factors. *Antioxid. Redox Signal.* **2011**, *15* (8), 2335–2381. https://doi.org/10.1089/ars.2010.3534.
(19) Savina, A.; Jancic, C.; Hugues, S.; Guermonprez, P.; Vargas, P.; Moura, I. C.; Lennon-Duménil, A.-M.; Seabra, M. C.; Raposo, G.; Amigorena, S. NOX2 Controls Phagosomal PH to Regulate Antigen Processing during Crosspresentation by Dendritic Cells. *Cell* **2006**, *126* (1), 205–218. https://doi.org/10.1016/j.cell.2006.05.035.
(20) Rehor, A.; Hubbell, J. A.; Tirelli, N. Oxidation-Sensitive Polymeric Nanoparticles. *Langmuir* **2005**, *21* (1), 411–417. https://doi.org/10.1021/la0478043.
(21) Toxicological Profile for Boron. *Agency for Toxic Substances and Disease Registry*; U.S. Department of Health and Human Services, 2010.
(22) McNaught, A. D.; Wilkinson, A. *IUPAC, Compendium of Chemical Terminology*, 2nd ed.; Blackwell Scientific Publications, 1997.
(23) Hall, D. G. *Boronic Acids : Preparation and Applications in Organic Synthesis, Medicine and Materials.*, 2nd ed.; John Wiley & Sons, Incorporated, 2011.
(24) Kuivila, H. G.; Keough, A. H.; Soboczenski, E. J. Areneboronates From Diols And Polyols1. *J. Org. Chem.* **1954**, *19* (5), 780–783. https://doi.org/10.1021/jo01370a013.
(25) Akgun, B.; Hall, D. G. Fast and Tight Boronate Formation for Click Bioorthogonal Conjugation. *Angew. Chem. Int. Ed. 55* (12), 3909–3913. https://doi.org/10.1002/anie.201510321.
(26) Kim, D.; Robyt, J. F.; Lee, S.-Y.; Lee, J.-H.; Kim, Y.-M. Dextran Molecular Size and Degree of Branching as a Function of Sucrose Concentration, PH, and Temperature of Reaction of Leuconostoc Mesenteroides B-512FMCM Dextransucrase. *Carbohydr. Res.* **2003**, *338* (11), 1183–1189. https://doi.org/10.1016/S0008-6215(03)00148-4.
(27) Collins, P. M. *Dictionary of Carbohydrates*, 2nd ed.; Chapman and Hall/CRC, 2005.
(28) Federation of American Societies for Experimental Biology.; United States. *Evaluation of the Health Aspects of Dextrans as Food Ingredients*; Life Sciences Research Office, Federation of American Societies of

Experimental Biology ; [available from] National Technical Information Service: Bethesda, Md. : Springfield, Va., 1975.
(29) Gray, A.; Wright, J.; Goodey, V.; Bruce, L. *Injectable Drugs Guide*, 1st ed.; Pharmaceutical Press, 2011.
(30) Cadée, J. A.; van Luyn, M. J. A.; Brouwer, L. A.; Plantinga, J. A.; van Wachem, P. B.; de Groot, C. J.; den Otter, W.; Hennink, W. E. In Vivo Biocompatibility of Dextran-Based Hydrogels. *J. Biomed. Mater. Res.* **2000**, *50* (3), 397–404. https://doi.org/10.1002/(SICI)1097-4636(20000605)50:3<397::AID-JBM14>3.0.CO;2-A.
(31) Broaders, K. E.; Grandhe, S.; Fréchet, J. M. J. A Biocompatible Oxidation-Triggered Carrier Polymer with Potential in Therapeutics. *J. Am. Chem. Soc.* **2011**, *133* (4), 756–758. https://doi.org/10.1021/ja110468v.
(32) Bao, J.; Wulff, W. D.; Dominy, J. B.; Fumo, M. J.; Grant, E. B.; Rob, A. C.; Whitcomb, M. C.; Yeung, S.-M.; Ostrander, R. L.; Rheingold, A. L. Synthesis, Resolution, and Determination of Absolute Configuration of a Vaulted 2,2‘-Binaphthol and a Vaulted 3,3‘-Biphenanthrol (VAPOL). *J. Am. Chem. Soc.* **1996**, *118* (14), 3392–3405. https://doi.org/10.1021/ja952018t.
(33) Zhang, Y.; Yeung, S.-M.; Wu, H.; Heller, D. P.; Wu, C.; Wulff, W. D. Highly Enantioselective Deracemization of Linear and Vaulted Biaryl Ligands. *Org. Lett.* **2003**, *5* (11), 1813–1816. https://doi.org/10.1021/ol0275769.
(34) Yu, S.; Rabalakos, C.; Mitchell, W. D.; Wulff, W. D. New Synthesis of Vaulted Biaryl Ligands via the Snieckus Phenol Synthesis. *Org. Lett.* **2005**, *7* (3), 367–369. https://doi.org/10.1021/ol047852e.
(35) Diemoz, K. M.; Wilson, S. O.; Franz, A. K. Synthesis of Structurally Varied 1,3-Disiloxanediols and Their Activity as Anion-Binding Catalysts. *Chem. – Eur. J.* **2016**, *22* (51), 18349–18353. https://doi.org/10.1002/chem.201604103.
(36) Matteson, D. S.; Man, H.-W. Hydrolysis of Substituted 1,3,2-Dioxaborolanes and an Asymmetric Synthesis of a Differentially Protected Syn,Syn-3-Methyl-2,4-Hexanediol. *J. Org. Chem.* **1996**, *61* (17), 6047–6051. https://doi.org/10.1021/jo960684m.
(37) Bernardini, R.; Oliva, A.; Paganelli, A.; Menta, E.; Grugni, M.; Munari, S. D.; Goldoni, L. Stability of Boronic Esters to Hydrolysis: A Comparative Study. *Chem. Lett.* **2009**, *38* (7), 750–751. https://doi.org/10.1246/cl.2009.750.
(38) Springsteen, G.; Wang, B. A Detailed Examination of Boronic Acid–Diol Complexation. *Tetrahedron* **2002**, *58* (26), 5291–5300. https://doi.org/10.1016/S0040-4020(02)00489-1.
(39) Roy, C. D.; Brown, H. C. A Study of Transesterification of Chiral (−)-Pinanediol Methylboronic Ester with Various Structurally Modified Diols. *Monatshefte Für Chem. - Chem. Mon.* **2007**, *138* (8), 747–753. https://doi.org/10.1007/s00706-007-0681-7.
(40) Roy, C. D.; Brown, H. C. A Comparative Study of the Relative Stability of Representative Chiral and Achiral Boronic Esters Employing

Transesterification. *Monatshefte Für Chem. - Chem. Mon.* **2007**, *138* (9), 879–887. https://doi.org/10.1007/s00706-007-0699-x.
(41) Donohoe, T. J.; Jahanshahi, A.; Tucker, M. J.; Bhatti, F. L.; Roslan, I. A.; Kabeshov, M.; Wrigley, G. Exerting Control over the Acyloin Reaction. *Chem. Commun.* **2011**, *47* (20), 5849–5851. https://doi.org/10.1039/C1CC11654A.
(42) Akgun, B.; Hall, D. G. Fast and Tight Boronate Formation for Click Bioorthogonal Conjugation. *Angew. Chem. Int. Ed. 55* (12), 3909–3913. https://doi.org/10.1002/anie.201510321.
(43) Pedersen, D. S.; Rosenbohm, C. Dry Column Vacuum Chromatography. *Synthesis* **2001**, *2001* (16), 2431–2434. https://doi.org/10.1055/s-2001-18722.
(44) Li, M.; Rouaud, O.; Poncelet, D. Microencapsulation by Solvent Evaporation: State of the Art for Process Engineering Approaches. *Int. J. Pharm.* **2008**, *363* (1), 26–39. https://doi.org/10.1016/j.ijpharm.2008.07.018.
(45) Iqbal, M.; Zafar, N.; Fessi, H.; Elaissari, A. Double Emulsion Solvent Evaporation Techniques Used for Drug Encapsulation. *Int. J. Pharm.* **2015**, *496* (2), 173–190. https://doi.org/10.1016/j.ijpharm.2015.10.057.
(46) Karatzas, I.; Shreve, S. E. Brownian Motion. In *Brownian Motion and Stochastic Calculus*; Karatzas, I., Shreve, S. E., Eds.; Springer New York: New York, NY, 1998; pp 47–127. https://doi.org/10.1007/978-1-4612-0949-2_2.
(47) Leyva, A.; Quintana, A.; Sánchez, M.; Rodríguez, E. N.; Cremata, J.; Sánchez, J. C. Rapid and Sensitive Anthrone–Sulfuric Acid Assay in Microplate Format to Quantify Carbohydrate in Biopharmaceutical Products: Method Development and Validation. *Biologicals* **2008**, *36* (2), 134–141. https://doi.org/10.1016/j.biologicals.2007.09.001.
(48) Beaudette, T. T.; Cohen, J. A.; Bachelder, E. M.; Broaders, K. E.; Cohen, J. L.; Engleman, E. G.; Fréchet, J. M. J. Chemoselective Ligation in the Functionalization of Polysaccharide-Based Particles. *J. Am. Chem. Soc.* **2009**, *131* (30), 10360–10361. https://doi.org/10.1021/ja903984s.
(49) Stockert, J. C.; Horobin, R. W.; Colombo, L. L.; Blázquez-Castro, A. Tetrazolium Salts and Formazan Products in Cell Biology: Viability Assessment, Fluorescence Imaging, and Labeling Perspectives. *Acta Histochem.* **2018**, *120* (3), 159–167. https://doi.org/10.1016/j.acthis.2018.02.005.
(50) Engvall, E.; Perlmann, P. Enzyme-Linked Immunosorbent Assay, Elisa. *J. Immunol.* **1972**, *109* (1), 129.
(51) Duong, A. D.; Sharma, S.; Peine, K. J.; Gupta, G.; Satoskar, A. R.; Bachelder, E. M.; Wyslouzil, B. E.; Ainslie, K. M. Electrospray Encapsulation of Toll-Like Receptor Agonist Resiquimod in Polymer Microparticles for the Treatment of Visceral Leishmaniasis. *Mol. Pharm.* **2013**, *10* (3), 1045–1055. https://doi.org/10.1021/mp3005098.
(52) Serda, R. Particle Platforms for Cancer Immunotherapy. *Int. J. Nanomedicine* **2013**, 1683. https://doi.org/10.2147/IJN.S31756.

Appendix

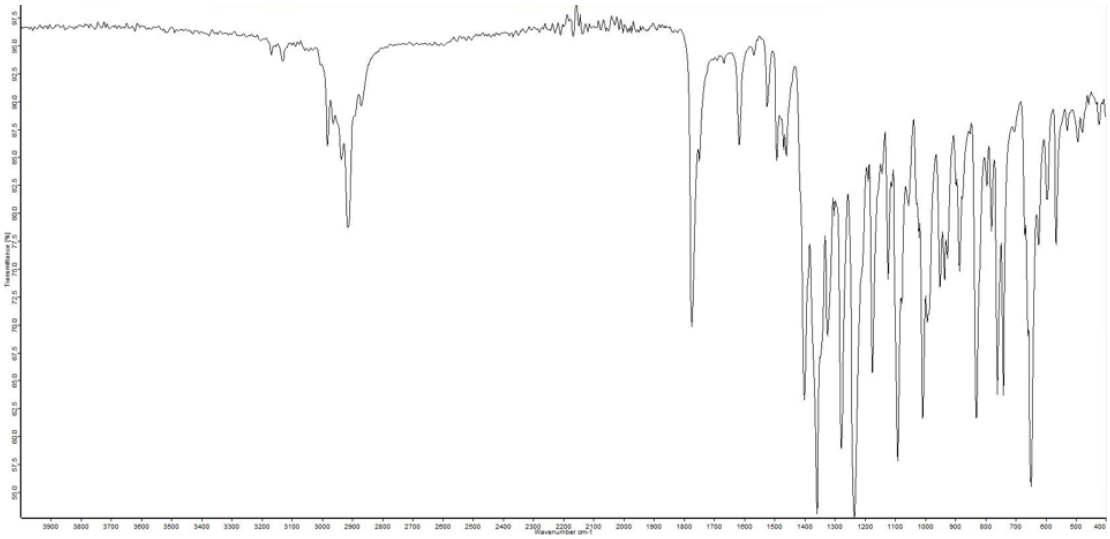

Figure A1. IR Spectrum of Pinane Boronate

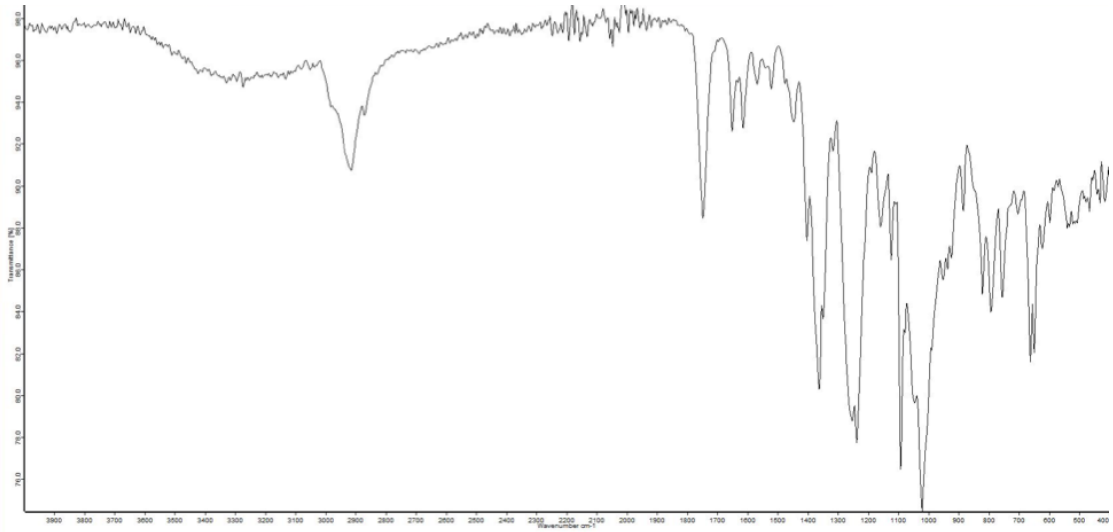

Figure A2. IR Spectrum of CDI-Activated Pinane Boronate

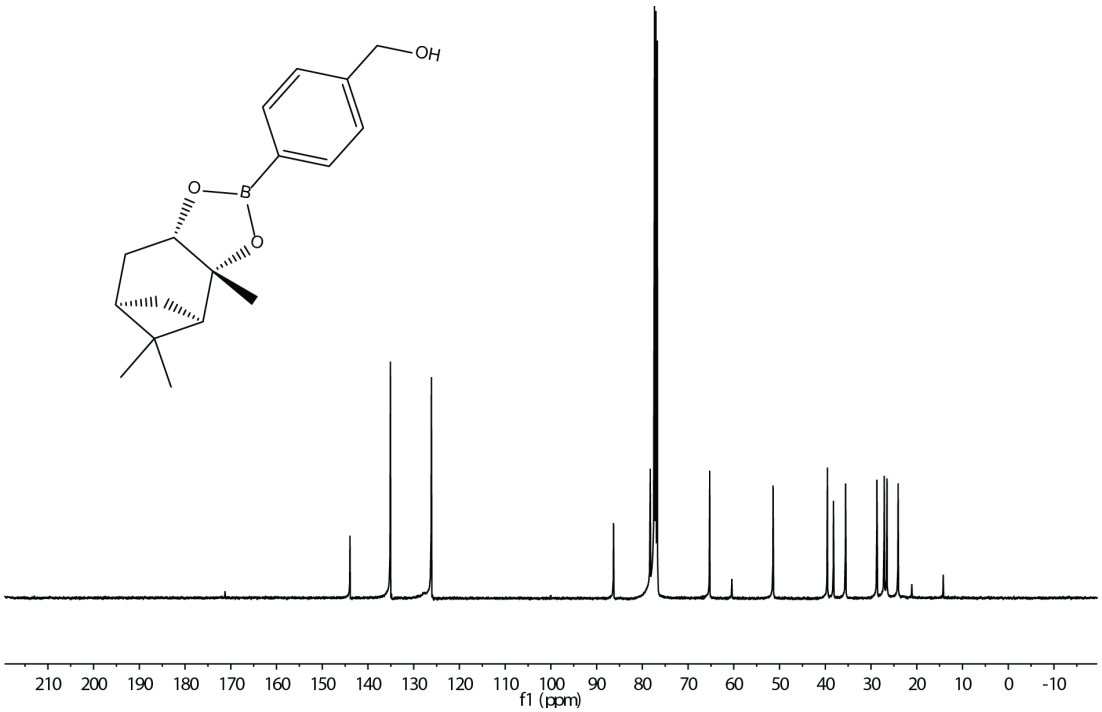

Figure A3. ^{13}C-NMR of Pinane Boronate

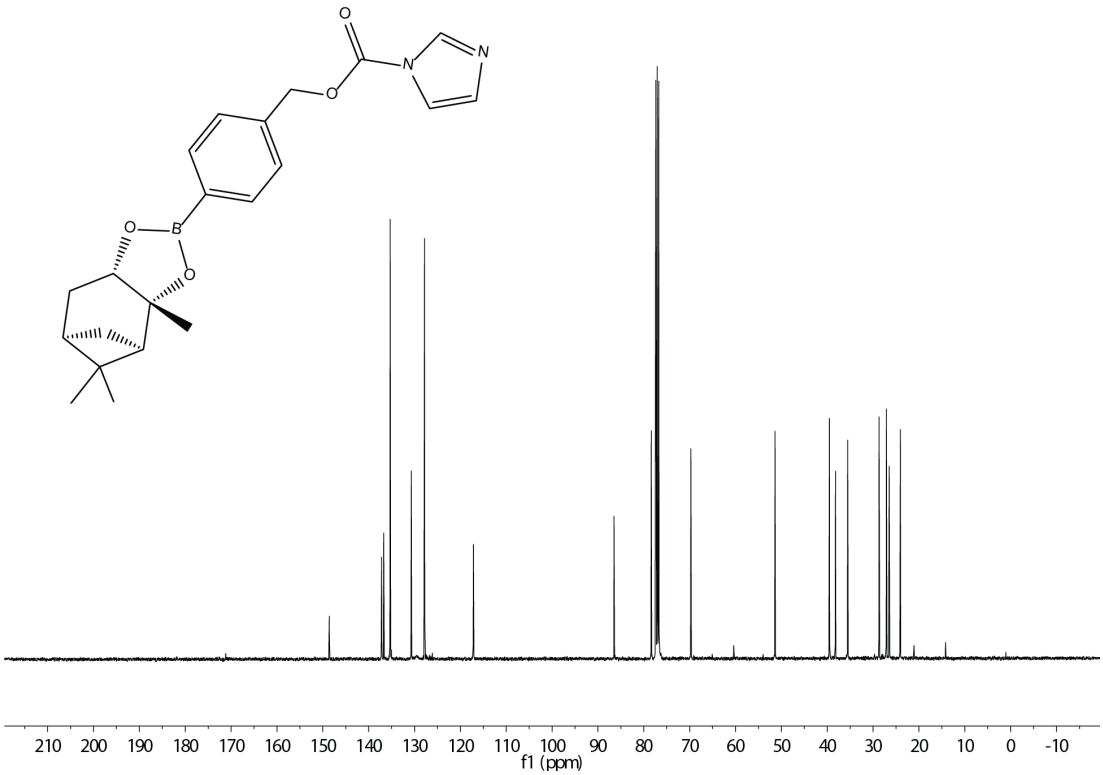

Figure A4. ^{13}C-NMR of CDI-Activated Pinane Boronat

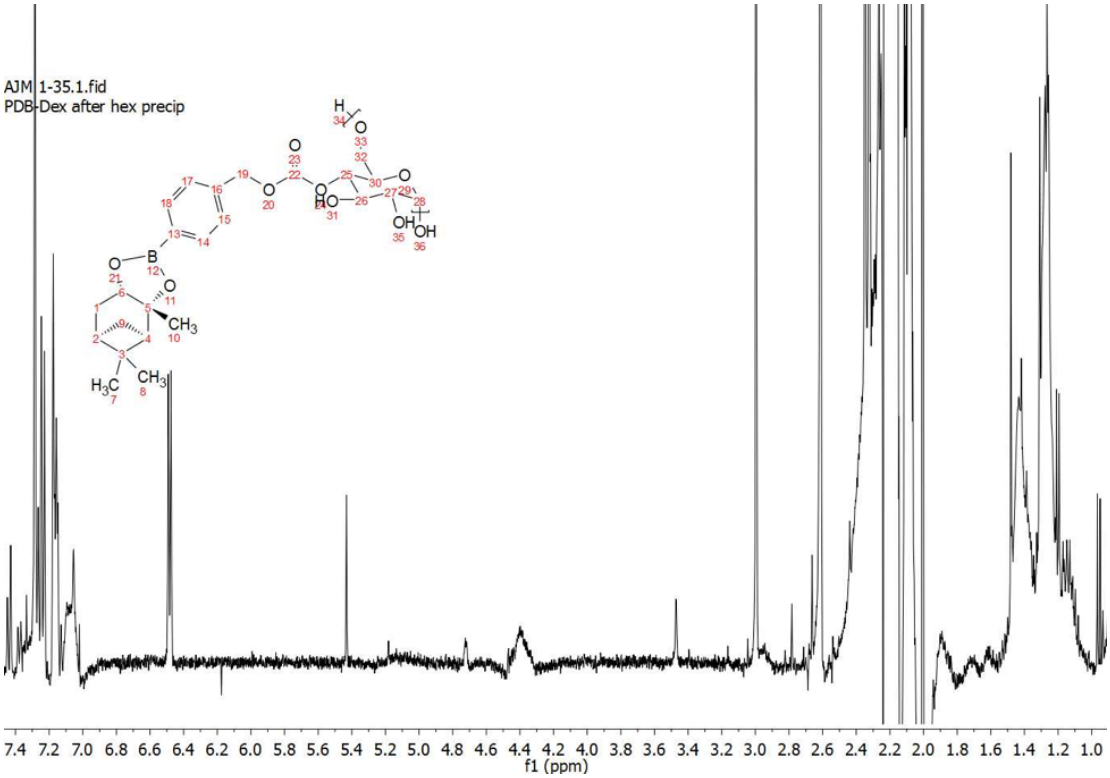

Figure A5. ^{1}H-NMR of PDB-Dex

A.1: Materials:

Unless otherwise specified all reagents were purchased from Sigma Aldrich, Acros Organics, or Oakwood Chemical and used without further purification without otherwise specified. Water (dd-H_2O) for buffers and particle washing steps was purified to a resistance of 18.2 MΩ using a Milli-Q Advance a10 purification system (Millipore, USA). ^{1}H spectra were recorded at 400 MHz and ^{13}C spectra were recorded at 100 MHz on a Bruker AVANCE II with BBI broadband probe and variable temperature unit. Infrared spectra were collected using a Bruker Alpha with ATR. Dynamic light scattering was performed using a Malvern Zetasizer Nano

ZS (Malvern, UK). A Branson SFX550 Ultrasonicator was used for particle preparation via single emulsion. Assays were analyzed using a SpectraMax M5e Multimode Plate Reader (Molecular Devices, USA). Lyophilization was done on a FreeZone 4.5 (Labconco, USA). THF and DCM were stored and dispensed from a PureSolv solvent purification system (Inert, USA). Large scale centrifugations (more than 1.5 mL) were done in a Sorvall Legend X1 with a fixed angle rotor (ThermoFisher Scientific, USA). Small scale centrifugations were done with a MiniSpin (Eppendorf, Germany). Phosphate buffered saline (PBS) was prepared to a pH of 7.4 at a concentration of 10 mM. Non-DCVC columns were run on a Biotage Isolera One.